

# On-manifold Decentralized State Estimation using Pseudomeasurements and Preintegration

Journal Title  
XX(X):1–15  
©The Author(s) 2023  
Reprints and permission:  
sagepub.co.uk/journalsPermissions.nav  
DOI: 10.1177/ToBeAssigned  
www.sagepub.com/

SAGE

Charles Champagne Cossette<sup>1</sup> and Mohammed Ayman Shalaby<sup>1</sup> and David Saussié<sup>2</sup> and James Richard Forbes<sup>1</sup>

## Abstract

This paper addresses the problem of decentralized, collaborative state estimation in robotic teams. In particular, this paper considers problems where individual robots estimate similar physical quantities, such as each other's position relative to themselves. The use of *pseudomeasurements* is introduced as a means of modelling such relationships between robots' state estimates, and is shown to be a tractable way to approach the decentralized state estimation problem. Moreover, this formulation easily leads to a general-purpose observability test that simultaneously accounts for measurements that robots collect from their own sensors, as well as the communication structure within the team. Finally, input preintegration is proposed as a communication-efficient way of sharing odometry information between robots, and the entire theory is appropriate for both vector-space and Lie-group state definitions. The proposed framework is evaluated on three different simulated problems, and one experiment involving three quadcopters.

## Keywords

Relative position estimation, collaborative localization, Lie groups, multi-robot systems, state estimation, preintegration

## 1 Introduction

Decentralized state estimation is a fundamental requirement for real-world multi-robot deployments. Whether the task is collaborative mapping, relative localization, or collaborative dead-reckoning, the multi-robot estimation problem seeks to estimate the state of each robot given *all* the measurements that each robot obtains locally. This problem is made difficult by the fact that not all robots can communicate with each other and, furthermore, that high-frequency sensor measurements would require substantial communication bandwidth to simply share across the team. The *centralized estimator* is a computing unit that can somehow collect all the sensor measurements on each robot, and then fuse them all to jointly estimate the states of every robot in one large system. Theoretically, the centralized estimator has the lowest possible estimation error variance, and all decentralized implementations attempt to match its performance.

A common approach is for robots to share their current state and associated covariance rather than of a history of measurement values (Julier and Uhlmann (1997); Julier (2001); Carrillo-Arce et al. (2013)). This approach has the benefit of low communication cost and fixed message size, but suffers from a well-known issue of not being able to compute cross-correlations between the robots' state estimates (Shalaby et al. (2021)). Furthermore, in certain problems, robots may be estimating the same physical quantities. As an example, consider two robots estimating each other's position, in addition to their own positions, as shown in Figure 1 (left). Their state vectors are both robots' positions, and therefore both seek to estimate the same physical quantities, a situation referred to here as *full state overlap*. When robot states have similar, if not

identical state definitions, it is straightforward to compute the error between their state estimates using simple subtraction. However, for more complicated problems, especially those with state definitions belonging to arbitrary Lie groups, a generalized measure of error between different robots' state estimates must be introduced.

### 1.1 Contributions

This paper has three main contributions.

First, a framework for decentralized state estimation is proposed that uses *pseudomeasurements*. This is shown to be a tractable and effective way to model any generic nonlinear relationship between robot state definitions, including full or partial state overlap as special cases. A pseudomeasurement is introduced for each edge in the communication graph, and the proposed framework also naturally leads to a novel observability test that takes into account both the local measurements obtained by each robot in addition to the communication structure between them.

Second, the use of preintegration is proposed as a means of sharing odometry information over an arbitrary duration of time, in a lossless matter. The naive solution is for robots to share a history of odometry measurements since the last time they communicated, which has processing, memory, and communication requirements that grow linearly with

<sup>1</sup>Department of Mechanical Engineering, McGill University

<sup>2</sup>Department of Electrical Engineering, Polytechnique Montréal

#### Corresponding author:

Charles Champagne Cossette, Department of Mechanical Engineering, McGill University, Montréal, Canada.

Email: charles.cossette@mail.mcgill.ca

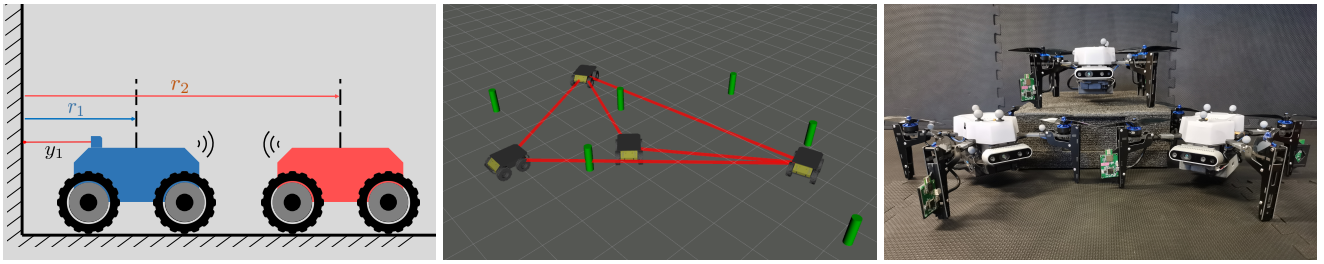


**Figure 1.** Three examples of decentralized estimation problems within the scope of this paper. **Left:** A toy problem with 1D robots, each estimating both of their positions. **Middle:** A problem with an incomplete communication graph. Robots observe landmarks, have range measurements to each other, and estimate their own and neighbor absolute poses. **Right:** A more complicated experimentally-tested problem, where robots equipped with ultra-wideband radios estimate both their own absolute pose and relative poses of neighbors, in addition to IMU biases.

the time interval between communications. Preintegration provides a constant-time, constant-memory, and constant-communication alternative that is algebraically identical to simply sharing the input measurements themselves. This makes preintegration a natural choice for multi-robot estimation problems. Moreover, preintegration preserves statistical independence assumptions that typical Kalman filtering prediction steps rely on. Preintegration is best known from the visual-inertial odometry literature (Lupton and Sukkarieh (2012); Forster et al. (2017)), where the same concept, adapted for relative pose estimation is introduced by Shalaby et al. (2023). This paper generalizes the concept to other common process models in robotics, presents a solution for simultaneous input bias estimation, and also further proposes a deep autoencoder to compress the associated covariance information.

Third, the theory here is developed for general on-manifold state definitions, including familiar linear vector spaces. The proposed solution is general to any state definition, process model, and measurement model subject to typical Gaussian noise assumptions.

This paper does not focus on the treatment of cross-correlations, and hence employs the simple, well-known covariance intersection (CI) (Julier and Uhlmann (1997); Julier (2001)) method. This allows for an arbitrary communication graph within the robot team, while remaining lightweight and avoiding cumbersome bookkeeping. The main drawback is that CI is proven to yield sub-optimal estimation. However, in practice, the performance can remain adequate, and sometimes very comparable to centralized estimation, as shown here from simulated and experimental results.

The remainder of this paper is as follows. Related work is discussed in Section 2 and mathematical preliminaries and notation are shown in Section 3. The paper then starts with a simplified “toy” problem showcasing the proposed method in Section 4, and the theory is generalized in Section 5. Preintegration sharing is presented in Section 6. Finally, Section 7 contains an application to a ground robot simulation, Section 8 applies the method to a more complicated experimental quadcopter problem.

## 2 Related Work

There are many sub-problems associated with the overall decentralized state estimation problem. Even if communication links between robots are assumed to be lossless and have infinite bandwidth, there is still the issue of propagating information over general, incomplete communication graphs. For two robots, it is straightforward to compute centralized-equivalent estimators on each robot as done by Grime and Durrant-Whyte (1994), which use information filters to accumulate the information from a series of measurements, and then communicate this quantity. Grime and Durrant-Whyte (1994) also derived centralized-equivalent solutions for fully connected graphs, as well as tree-shaped graphs. However, they show that for generic graphs, it is impossible to obtain a centralized-equivalent estimate with only neighboring knowledge, and that more knowledge of the graph topology is required.

Leung et al. (2010) present a general centralized-equivalent algorithm for arbitrary time-varying graphs, and is formulated over distributions directly, hence allowing inference using any algorithm such as an extended or sigma-point Kalman filter. Robots must still share raw measurements with each other, therefore requiring substantial bookkeeping. The approach is extended to the SLAM problem by Leung et al. (2012). Roumeliotis and Bekey (2002) decompose the centralized Kalman filter equations using a singular value decomposition to generate independent equations that each robot can compute. Provided that robots have broadcasting ability, and obtain direct pose measurements of their neighbors, a centralized-equivalent solution can be obtained. The consensus Kalman filter (Olfati-Saber and Murray (2004); Olfati-Saber (2005)) aims to asymptotically send the state of  $n$  arbitrary nodes to a common value, which is effectively a problem with full state overlap. Battistelli et al. (2015) proposes alternate consensus approaches such as “consensus on information” or “consensus on measurements”. However, the problem does not consider the fact that robots collect their own, separate odometry measurements that are not necessarily available to neighboring robots.

As previously mentioned, one of the simplest solutions to the decentralized estimation problem is to use covariance intersection (Julier and Uhlmann (1997); Julier (2001)). CI conservatively assumes maximum correlation between robot estimates. Although the performance is theoretically suboptimal, the implementation is extremely simple, and

imposes no constraints whatsoever on the communication frequency or graph topology. Carrillo-Arce et al. (2013) apply covariance intersection to a collaborative localization problem, where each robot estimates their own absolute state given direct relative pose measurements to other robots. Recently, Li and Yang (2021) exploit covariance intersection for the fusion of poses on Lie groups. Luft et al. (2018) use an EKF-like filter for decentralized estimation where cross-correlations are also explicitly tracked for both the prediction step and the fusion of local measurements. When relative measurements are encountered, an improved approximation to the joint covariance matrix is developed, which outperforms CI. The approach of Luft et al. (2018) assumes that process model inputs between robots are uncorrelated, which is not applicable in some of the problems in this paper. The work by Jung et al. (2020) builds off of Luft et al. (2018) to solve a full 3D collaborative state estimation problem where each robot has a camera and an IMU.

Another approach using scattering theory has recently been presented for two robots (Allak et al. (2019, 2022)), with the objective of reducing the communication cost associated with high-rate sensor measurements. Also making reference to the IMU preintegration technique (Lupton and Sukkarieh (2012); Forster et al. (2017)), covariance pre-computations are derived by Allak et al. (2019) and later extended to also include the mean (Allak et al. (2022)). It is shown that by sharing pre-computed matrices with twice the size as the state vector, a centralized-equivalent state estimate can be directly obtained with no measurement reprocessing. However, the generalization to more robots does not seem straightforward.

### 3 Preliminaries

This paper will address problems where an individual robot's motion and measurements are modelled in the standard form of

$$\begin{aligned} \mathcal{X}_{i_k} &= \mathbf{f}(\mathcal{X}_{i_{k-1}}, \mathbf{u}_{i_{k-1}}, \mathbf{w}_{i_{k-1}}), & \mathbf{w}_{i_{k-1}} &\sim \mathcal{N}(\mathbf{0}, \mathbf{Q}_{i_{k-1}}), \\ \mathbf{y}_{i_k} &= \mathbf{g}(\mathcal{X}_{i_k}) + \mathbf{v}_{i_k}, & \mathbf{v}_{i_k} &\sim \mathcal{N}(\mathbf{0}, \mathbf{R}_{i_k}), \end{aligned} \quad (1)$$

for Robot  $i$ , where  $\mathbf{u}_{i_k} \in \mathbb{R}^{n_u}$  is the process input at time step  $k$ ,  $\mathbf{y}_{i_k} \in \mathbb{R}^{n_y}$  are the measurements, and  $\mathcal{X}_{i_k} \in G$  denotes the robot state belonging to any Lie group  $G$ . As a notational convenience, the shorthand  $\mathcal{X}_{i:j} = \{\mathcal{X}_i \dots \mathcal{X}_j\}$  will refer to a collection of arbitrary objects with indices in the range  $[i, j]$ .

#### 3.1 Lie groups

A Lie group  $G$  is a smooth manifold whose elements, given a group operation  $\circ : G \times G \rightarrow G$ , satisfy the group axioms (Solà et al. (2018)). The application of this operation to two arbitrary group elements  $\mathcal{X}, \mathcal{Y} \in G$  is written as  $\mathcal{X} \circ \mathcal{Y} \in G$ . For any  $G$ , there exists an associated Lie algebra  $\mathfrak{g}$ , a vector space identifiable with elements of  $\mathbb{R}^m$ , where  $m$  is referred to as the degrees of freedom of  $G$ . Lie algebra elements are related to group elements through the exponential and logarithmic maps, denoted  $\exp : \mathfrak{g} \rightarrow G$  and  $\log : G \rightarrow \mathfrak{g}$ . The “vee” and “wedge” operators are denoted  $(\cdot)^\vee : \mathfrak{g} \rightarrow \mathbb{R}^m$  and  $(\cdot)^\wedge : \mathbb{R}^m \rightarrow \mathfrak{g}$ , which can be used to associate Lie algebra elements with vectors. Composing these operators,

group elements can be associated with vectors using

$$\mathcal{X} = \exp(\boldsymbol{\xi}^\wedge) \triangleq \text{Exp}(\boldsymbol{\xi}), \quad \boldsymbol{\xi} = \log(\mathcal{X})^\vee \triangleq \text{Log}(\mathcal{X}),$$

where  $\mathcal{X} \in G$ ,  $\boldsymbol{\xi} \in \mathbb{R}^m$ , and the shorthand notation  $\text{Exp} : \mathbb{R}^m \rightarrow G$  and  $\text{Log} : G \rightarrow \mathbb{R}^m$  has been defined. Following Solà et al. (2018), the adjoint matrix representation of an element  $\mathcal{X} \in G$  is denoted  $\text{Ad} : G \rightarrow \mathbb{R}^{m \times m}$  and defined such that

$$\text{Ad}(\mathcal{X})\boldsymbol{\xi} = (\mathcal{X}\boldsymbol{\xi}^\wedge\mathcal{X}^{-1})^\vee.$$

The most common Lie groups appearing in robotics are  $SO(n)$ , representing rotations in  $n$ -dimensional space,  $SE(n)$ , representing poses, and  $SE_2(3)$  representing “extended” poses that also contain velocity information. In these cases, the elements  $\mathcal{X}$  are invertible matrices and the group operation  $\circ$  is regular matrix multiplication.

**3.1.1  $\oplus$  and  $\ominus$  operators.** Estimation theory for vector-space states and Lie groups can be elegantly aggregated into a single mathematical treatment by defining generalized “addition”  $\oplus : G \times \mathbb{R}^m \rightarrow G$  and “subtraction”  $\ominus : G \times G \rightarrow \mathbb{R}^m$  operators, whose precise definitions will depend on the problem at hand. For example, possible implementations include

$$\begin{aligned} \mathcal{X} \oplus \delta\mathbf{x} &= \mathcal{X} \circ \text{Exp}(\delta\mathbf{x}) && \text{(Lie group right),} \\ \mathcal{X} \oplus \delta\mathbf{x} &= \text{Exp}(\delta\mathbf{x}) \circ \mathcal{X} && \text{(Lie group left),} \\ \mathbf{x} \oplus \delta\mathbf{x} &= \mathbf{x} + \delta\mathbf{x} && \text{(vector space),} \end{aligned}$$

for addition and, correspondingly,

$$\begin{aligned} \mathcal{X} \ominus \mathcal{Y} &= \text{Log}(\mathcal{Y}^{-1} \circ \mathcal{X}) && \text{(Lie group right),} \\ \mathcal{X} \ominus \mathcal{Y} &= \text{Log}(\mathcal{X} \circ \mathcal{Y}^{-1}) && \text{(Lie group left),} \\ \mathbf{x} \ominus \mathbf{y} &= \mathbf{x} - \mathbf{y} && \text{(vector space),} \end{aligned}$$

for subtraction. This abstraction is natural since a vector space technically qualifies as a Lie group with regular addition  $+$  as the group operation.

**3.1.2 Gaussian distributions on Lie groups.** As an example use of this abstraction, consider defining a normally-distributed Lie group element with mean  $\bar{\mathcal{X}}$  and covariance  $\boldsymbol{\Sigma}$ , as done by Barfoot and Furgale (2014), with

$$\mathcal{X} = \bar{\mathcal{X}} \circ \text{Exp}(\delta\mathbf{x}), \quad \delta\mathbf{x} \sim \mathcal{N}(\mathbf{0}, \boldsymbol{\Sigma}),$$

when using a right parameterization, or a similar definition for left parameterizations. This can alternatively be written in an abstract way, applicable to any group or vector space, with

$$\mathcal{X} = \bar{\mathcal{X}} \oplus \delta\mathbf{x}, \quad \delta\mathbf{x} \sim \mathcal{N}(\mathbf{0}, \boldsymbol{\Sigma}). \quad (2)$$

Moreover, given that  $\delta\mathbf{x} = \mathcal{X} \ominus \bar{\mathcal{X}}$ , it follows from (2) that

$$p(\mathcal{X}) = \eta \exp\left(-\frac{1}{2}(\mathcal{X} \ominus \bar{\mathcal{X}})^\top \boldsymbol{\Sigma}^{-1}(\mathcal{X} \ominus \bar{\mathcal{X}})\right) \triangleq \mathcal{N}_L(\bar{\mathcal{X}}, \boldsymbol{\Sigma}),$$

where the reader should note the definition of the generalized Gaussian  $\mathcal{N}_L(\bar{\mathcal{X}}, \boldsymbol{\Sigma})$ .

**3.1.3 Derivatives on Lie groups.** Again following Solà et al. (2018), the Jacobian of a function  $f : G \rightarrow G$ , taken with respect to  $\mathcal{X}$  can be defined as

$$\left. \frac{Df(\mathcal{X})}{D\mathcal{X}} \right|_{\bar{\mathcal{X}}} \triangleq \left. \frac{\partial f(\bar{\mathcal{X}} \oplus \delta\mathbf{x}) \ominus f(\bar{\mathcal{X}})}{\partial \delta\mathbf{x}} \right|_{\delta\mathbf{x}=\mathbf{0}}, \quad (3)$$

where it should be noted that the function  $f(\bar{\mathcal{X}} \oplus \delta \mathbf{x}) \ominus f(\bar{\mathcal{X}})$  of  $\delta \mathbf{x}$  has  $\mathbb{R}^m$  as both its domain and codomain, and can thus be differentiated using any standard technique. With the above general definition of a derivative, it is easy to define the so-called *Jacobian of  $G$*  as  $\mathbf{J} = D\text{Exp}(\mathbf{x})/D\mathbf{x}$ , where left/right group Jacobians are obtained with left/right definitions of  $\oplus$  and  $\ominus$ .

**3.1.4 Composite groups.** A *composite group* is simply the concatenation of  $N$  other Lie groups  $G_1, \dots, G_N$  (Solà et al. (2018)), with elements of the form

$$\mathcal{X} = (\mathcal{X}_1, \dots, \mathcal{X}_N) \in G_1 \times \dots \times G_N.$$

The group operation, inverse, and identity are defined elementwise. For example,

$$\mathcal{X} \circ \mathcal{Y} = (\mathcal{X}_1 \circ \mathcal{Y}_1, \dots, \mathcal{X}_N \circ \mathcal{Y}_N).$$

Furthermore, defining  $\delta \mathbf{x} = [\delta \mathbf{x}_1^\top \dots \delta \mathbf{x}_N^\top]^\top$  the  $\oplus$ , operator is given by

$$\mathcal{X} \oplus \delta \mathbf{x} = (\mathcal{X}_1 \oplus \delta \mathbf{x}_1, \dots, \mathcal{X}_N \oplus \delta \mathbf{x}_N)$$

and a similar definition applies to  $\ominus$ .

### 3.2 Maximum A Posteriori

*Maximum a posteriori* (MAP) is the standard approach taken in the robotics literature. Popular algorithms such as the extended Kalman filter (EKF), iterated EKF, sliding-window filter, and batch estimator can all be derived from a MAP approach, thus unifying them under a common theory. Given a measurement  $\mathbf{y}$  with a standard model as in (1), as well as a prior distribution  $p(\mathcal{X}) = \mathcal{N}_L(\bar{\mathcal{X}}, \hat{\mathbf{P}})$ , the estimate  $\hat{\mathcal{X}}$  produced by the MAP approach is

$$\begin{aligned} \hat{\mathcal{X}} &= \underset{\mathcal{X}}{\text{argmax}} p(\mathcal{X}|\mathbf{y}) \\ &= \underset{\mathcal{X}}{\text{argmax}} \eta p(\mathbf{y}|\mathcal{X})p(\mathcal{X}) \\ &= \underset{\mathcal{X}}{\text{argmax}} \eta \mathcal{N}(\mathbf{g}(\mathcal{X}), \mathbf{R}) \mathcal{N}_L(\bar{\mathcal{X}}, \hat{\mathbf{P}}) \end{aligned}$$

where  $\eta$  is a normalization constant. Equivalently, minimizing the negative logarithm yields a nonlinear least-squares problem of the form

$$\begin{aligned} \hat{\mathcal{X}} &= \underset{\mathcal{X}}{\text{argmax}} \frac{1}{2} \mathbf{e}(\mathcal{X})^\top \mathbf{W} \mathbf{e}(\mathcal{X}), \quad (4) \\ \mathbf{e}(\mathcal{X}) &= \begin{bmatrix} \mathcal{X} \ominus \bar{\mathcal{X}} \\ \mathbf{y} - \mathbf{g}(\mathcal{X}) \end{bmatrix}, \end{aligned}$$

where  $\mathbf{W} = \text{diag}(\hat{\mathbf{P}}^{-1}, \mathbf{R}^{-1})$ . Using an on-manifold optimization approach, (4) can be solved by first parameterizing the state with  $\mathcal{X} = \bar{\mathcal{X}} \oplus \delta \mathbf{x}$  and solving the problem

$$\delta \hat{\mathbf{x}} = \underset{\delta \mathbf{x}}{\text{argmax}} \frac{1}{2} \mathbf{e}(\bar{\mathcal{X}} \oplus \delta \mathbf{x})^\top \mathbf{W} \mathbf{e}(\bar{\mathcal{X}} \oplus \delta \mathbf{x}). \quad (5)$$

Using (3), the Jacobian of the error vector is given by

$$\mathbf{H} \triangleq \left. \frac{D\mathbf{e}(\mathcal{X})}{D\mathcal{X}} \right|_{\bar{\mathcal{X}}} = \left. \frac{\partial \mathbf{e}(\bar{\mathcal{X}} \oplus \delta \mathbf{x})}{\partial \delta \mathbf{x}} \right|_{\delta \mathbf{x}=\mathbf{0}},$$

and an approximate solution to (5) can be obtained by solving the Gauss-Newton system

$$(\mathbf{H}^\top \mathbf{W} \mathbf{H}) \delta \hat{\mathbf{x}} = \mathbf{H}^\top \mathbf{W} \mathbf{e}(\bar{\mathcal{X}}).$$

The above is iterated with  $\hat{\mathcal{X}} \leftarrow \bar{\mathcal{X}} \oplus \delta \hat{\mathbf{x}}$  and initialized with  $\hat{\mathcal{X}} \leftarrow \bar{\mathcal{X}}$ . A common approximation for the posterior covariance  $\hat{\mathbf{P}}$  where  $p(\mathcal{X}|\mathbf{y}) \approx \mathcal{N}_L(\hat{\mathcal{X}}, \hat{\mathbf{P}})$  is given by  $\hat{\mathbf{P}} = (\mathbf{H}^\top \mathbf{W} \mathbf{H})^{-1}$  with  $\mathbf{H}$  evaluated at  $\hat{\mathcal{X}}$ .

### 3.3 Covariance Intersection

Covariance intersection (CI) is a tool introduced by Julier and Uhlmann (1997) for the purposes of decentralized data fusion under unknown cross-correlations, and can be summarized with the following theorem.

**Theorem 1.** Consistency of Covariance Intersection. *The inequality*

$$\begin{bmatrix} \frac{1}{w} \Sigma_{xx} & \mathbf{0} \\ \mathbf{0} & \frac{1}{1-w} \Sigma_{yy} \end{bmatrix} \geq \begin{bmatrix} \Sigma_{xx} & \Sigma_{xy} \\ \Sigma_{xy}^\top & \Sigma_{yy} \end{bmatrix}, \quad (6)$$

which applies in the positive definite sense, holds for all  $w \in (0, 1)$ , where  $\Sigma_{xx}$ ,  $\Sigma_{yy}$ , and the right-hand-side of (6) are positive definite.

## 4 A Toy Problem

Consider first one of the simplest multi-robot estimation problems, shown on the left of Figure 1. Two robots are located at positions  $r_1$  and  $r_2$ , respectively, and both robots seek to estimate both robots' positions. By design, each robot carries distinct, conceptually independent estimates, even though their states represent the same true *physical* variables. This mimics exactly what will occur in implementation, as each robot's processor will have a live estimate of both robots' positions. Their state vectors can therefore be defined as

$$\mathbf{x}_1 = \begin{bmatrix} r_1^{[1]} & r_2^{[1]} \end{bmatrix}^\top, \quad \mathbf{x}_2 = \begin{bmatrix} r_1^{[2]} & r_2^{[2]} \end{bmatrix}^\top,$$

where the square bracket superscript  $(\cdot)^{[i]}$  is used when necessary to denote Robot  $i$ 's estimate or "instance" of a common physical variable. Each robot also collects local measurements from its sensors. Robot 1 is capable of measuring its own position,

$$y_1 = \mathbf{G}_1 \mathbf{x}_1 + v_1, \quad v_1 \sim \mathcal{N}(0, R_1), \quad \mathbf{G}_1 = \begin{bmatrix} 1 & 0 \end{bmatrix},$$

while Robot 2 is only capable of measuring its position relative to Robot 1,

$$y_2 = \mathbf{G}_2 \mathbf{x}_2 + v_2, \quad v_2 \sim \mathcal{N}(0, R_2), \quad \mathbf{G}_2 = \begin{bmatrix} -1 & 1 \end{bmatrix}.$$

To keep things simple for this demonstrative problem, robots are assumed to have access to each other's input measurements, such as wheel odometry. This allows them to predict their state forward in time using a conventional Kalman filter. However, a more communication-efficient solution will be proposed in Section 6. Neither robot is capable of estimating their full state vector from local measurements only, meaning that some form of communication will be required.



To reflect the knowledge that the two robots' state vectors are physically the same, a key design choice of this paper is to incorporate a *pseudomeasurement* of the form

$$\mathbf{y}_{12} = \mathbf{x}_1 - \mathbf{x}_2 + \mathbf{v}_{12}, \quad \mathbf{v}_{12} \sim \mathcal{N}(\mathbf{0}, \Psi),$$

whose "measured" value is always exactly zero. This pseudomeasurement can be viewed as a soft constraint on the problem, inversely weighted by the user-chosen pseudomeasurement covariance  $\Psi$ . The estimation problem is now to compute, as accurately as possible, the posterior distribution

$$p(\mathbf{x}_1, \mathbf{x}_2 | \mathbf{y}_1, \mathbf{y}_2, \mathbf{y}_{12}).$$

#### 4.1 Solution via MAP

Applying MAP to this simplified problem is to say that

$$\hat{\mathbf{x}}_1, \hat{\mathbf{x}}_2 = \underset{\mathbf{x}_1, \mathbf{x}_2}{\operatorname{argmax}} p(\mathbf{x}_1, \mathbf{x}_2 | \mathbf{y}_1, \mathbf{y}_2, \mathbf{y}_{12}). \quad (7)$$

Assuming that  $\mathbf{v}_1, \mathbf{v}_2, \mathbf{v}_{12}$  are all independent random variables allows the use of Bayes' rule to write

$$p(\mathbf{x}_1, \mathbf{x}_2 | \mathbf{y}_1, \mathbf{y}_2, \mathbf{y}_{12}) = \eta p(\mathbf{y}_1 | \mathbf{x}_1) p(\mathbf{y}_2 | \mathbf{x}_2) \times p(\mathbf{y}_{12} | \mathbf{x}_1, \mathbf{x}_2) p(\mathbf{x}_1, \mathbf{x}_2). \quad (8)$$

Next, assume that the prior distributions of the robots are independent and Gaussian, possibly as a result of using CI,

$$p(\mathbf{x}_1, \mathbf{x}_2) = p(\mathbf{x}_1) p(\mathbf{x}_2) = \mathcal{N}(\tilde{\mathbf{x}}_1, \tilde{\mathbf{P}}_1) \mathcal{N}(\tilde{\mathbf{x}}_2, \tilde{\mathbf{P}}_2). \quad (9)$$

Substituting (9) into (8) and grouping terms into those available to each robot yields

$$p(\mathbf{x}_1, \mathbf{x}_2 | \mathbf{y}_1, \mathbf{y}_2, \mathbf{y}_{12}) = \eta p(\mathbf{y}_{12} | \mathbf{x}_1, \mathbf{x}_2) \left( p(\mathbf{y}_1 | \mathbf{x}_1) p(\mathbf{x}_1) \right) \left( p(\mathbf{y}_2 | \mathbf{x}_2) p(\mathbf{x}_2) \right). \quad (10)$$

Since the local measurement models are linear, it is straightforward to exactly compute the terms

$$p(\mathbf{y}_i | \mathbf{x}_i) p(\mathbf{x}_i) = \eta_i p(\mathbf{x}_i | \mathbf{y}_i) = \eta_i \mathcal{N}(\tilde{\mathbf{x}}_i, \tilde{\mathbf{P}}_i), \quad i = 1, 2, \quad (11)$$

using the regular Kalman filter equations. The means and covariances  $\tilde{\mathbf{x}}_i, \tilde{\mathbf{P}}_i$  (with tildes) represent the distribution of each robot's state conditioned on only local measurements, without the information that the robots' states are physically the same. Substituting (11) into (10) yields a simplified expression for the posterior, and the optimization problem (7) now leads to the least-squares problem

$$\hat{\mathbf{x}}_1, \hat{\mathbf{x}}_2 = \underset{\mathbf{x}_1, \mathbf{x}_2}{\operatorname{argmin}} \frac{1}{2} \mathbf{e}(\mathbf{x}_1, \mathbf{x}_2)^\top \mathbf{W} \mathbf{e}(\mathbf{x}_1, \mathbf{x}_2),$$

where

$$\mathbf{e}(\mathbf{x}_1, \mathbf{x}_2) = \begin{bmatrix} \mathbf{1} & \mathbf{0} \\ \mathbf{0} & \mathbf{1} \\ \mathbf{1} & -\mathbf{1} \end{bmatrix} \begin{bmatrix} \mathbf{x}_1 \\ \mathbf{x}_2 \end{bmatrix} - \begin{bmatrix} \tilde{\mathbf{x}}_1 \\ \tilde{\mathbf{x}}_2 \\ \mathbf{0} \end{bmatrix} \triangleq \mathbf{H} \mathbf{x} - \mathbf{z},$$

$$\mathbf{W} = \operatorname{diag}(\tilde{\mathbf{P}}_1^{-1}, \tilde{\mathbf{P}}_2^{-1}, \Psi^{-1}).$$

In this linear case the unique solution  $\hat{\mathbf{x}}$  is given by

$$\hat{\mathbf{x}} = (\mathbf{H}^\top \mathbf{W} \mathbf{H})^{-1} \mathbf{H}^\top \mathbf{W} \mathbf{z}, \quad (12)$$

where

$$\mathbf{H}^\top \mathbf{W} \mathbf{H} = \begin{bmatrix} \tilde{\mathbf{P}}_1^{-1} + \Psi^{-1} & -\Psi^{-1} \\ -\Psi^{-1} & \tilde{\mathbf{P}}_2^{-1} + \Psi^{-1} \end{bmatrix},$$

$$\mathbf{H}^\top \mathbf{W} \mathbf{z} = \begin{bmatrix} \tilde{\mathbf{P}}_1^{-1} \tilde{\mathbf{x}}_1 \\ \tilde{\mathbf{P}}_2^{-1} \tilde{\mathbf{x}}_2 \end{bmatrix}.$$

Various applications of the Sherman-Morrison-Woodbury (SMW) identities can be used to analytically invert the information matrix  $\mathbf{H}^\top \mathbf{W} \mathbf{H}$ , as well as solve for the mean  $\hat{\mathbf{x}}$  in (12). After some manipulation, the result is

$$\hat{\mathbf{x}} \triangleq \begin{bmatrix} \hat{\mathbf{x}}_1 \\ \hat{\mathbf{x}}_2 \end{bmatrix} = \begin{bmatrix} \tilde{\mathbf{x}}_1 + \mathbf{K}_1(\tilde{\mathbf{x}}_2 - \tilde{\mathbf{x}}_1) \\ \tilde{\mathbf{x}}_2 + \mathbf{K}_2(\tilde{\mathbf{x}}_1 - \tilde{\mathbf{x}}_2) \end{bmatrix},$$

$$\hat{\mathbf{P}} \triangleq (\mathbf{H}^\top \mathbf{W} \mathbf{H})^{-1}$$

$$= \begin{bmatrix} (\mathbf{1} - \mathbf{K}_1) \tilde{\mathbf{P}}_1 & -\mathbf{K}_1 \tilde{\mathbf{P}}_2 \\ -\mathbf{K}_2 \tilde{\mathbf{P}}_1 & (\mathbf{1} - \mathbf{K}_2) \tilde{\mathbf{P}}_2 \end{bmatrix}, \quad (13)$$

$$\mathbf{K}_1 \triangleq \tilde{\mathbf{P}}_1 (\Psi + \tilde{\mathbf{P}}_2 + \tilde{\mathbf{P}}_1)^{-1},$$

$$\mathbf{K}_2 \triangleq \tilde{\mathbf{P}}_2 (\Psi + \tilde{\mathbf{P}}_2 + \tilde{\mathbf{P}}_1)^{-1},$$

and hence that  $p(\mathbf{x}_1, \mathbf{x}_2 | \mathbf{y}_1, \mathbf{y}_2, \mathbf{y}_{12}) = \mathcal{N}(\hat{\mathbf{x}}, \hat{\mathbf{P}})$ . The final individual estimates are obtained by marginalizing out the other robots' states, which is trivial to do in covariance form by simply extracting the corresponding blocks from  $\hat{\mathbf{x}}, \hat{\mathbf{P}}$ , yielding

$$p(\mathbf{x}_1 | \mathbf{y}_1, \mathbf{y}_2, \mathbf{y}_{12}) = \mathcal{N}(\hat{\mathbf{x}}_1, (\mathbf{1} - \mathbf{K}_1) \tilde{\mathbf{P}}_1),$$

$$p(\mathbf{x}_2 | \mathbf{y}_1, \mathbf{y}_2, \mathbf{y}_{12}) = \mathcal{N}(\hat{\mathbf{x}}_2, (\mathbf{1} - \mathbf{K}_2) \tilde{\mathbf{P}}_2).$$

Conditioning on the pseudomeasurement  $\mathbf{y}_{12}$  has introduced cross-correlation terms in (13), which are feasible to keep track of for this two-robot scenario, but introduce substantial complexity for an arbitrary multi-robot scenario. Therefore, this paper simply employs the CI approximation as required. Figure 2 shows the estimation error of each robot as multiple pseudomeasurements are fused in succession. The two robots' estimates not only converge to zero error, but also to a common value, which is the main effect of the pseudomeasurement. In Figure 3, 100 Monte-Carlo trials are performed on a simulation of this toy problem, but extended to four robots. The root-mean-squared error (RMSE) and normalized estimation error squared (NEES), calculated as per (Bar-Shalom et al. 2001, Ch. 5.4), are plotted through time. The lines marked "Proposed" fuse pseudomeasurements as described, and use CI before each state fusion. The naive solution is identical, but does not utilize covariance intersection before state fusion, thus completely neglects cross-correlations. Although the use of CI does introduce error compared to the centralized solution, it is still vastly better than the naive approach.

## 5 General Problem

Consider now  $N$  robots, which communicate in correspondence with an arbitrary undirected graph  $\mathcal{G} = (\mathcal{V}, \mathcal{E})$  where  $\mathcal{V} = \{1, \dots, N\}$  is the set of nodes or robot IDs, and  $\mathcal{E}$  is the set of edges. The robots have states  $\mathcal{X}_i \in G_i$ ,  $i \in \mathcal{V}$  belonging to possibly different groups. Pseudomeasurement models  $\mathbf{c}_{ij} : G_i \times G_j \rightarrow \mathbb{R}^c$  are now defined in a generic way

$$\mathbf{y}_{ijk} = \mathbf{c}_{ij}(\mathcal{X}_{i_k}, \mathcal{X}_{j_k}) + \mathbf{v}_{ijk}, \quad \mathbf{v}_{ijk} \sim \mathcal{N}(\mathbf{0}, \Psi),$$

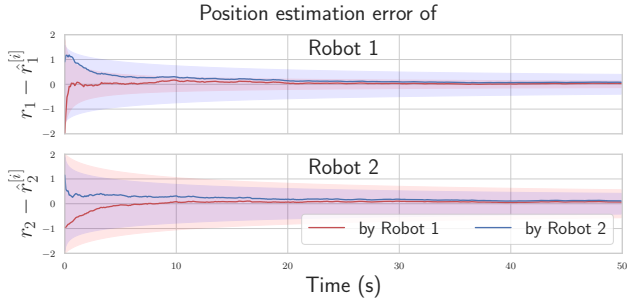


**Figure 2.** Estimation convergence for a single trial of the two-robot toy problem with  $\Psi = 10 \cdot \mathbf{1}$ . Due to pseudomeasurements, the robot states successfully converge to a common value.

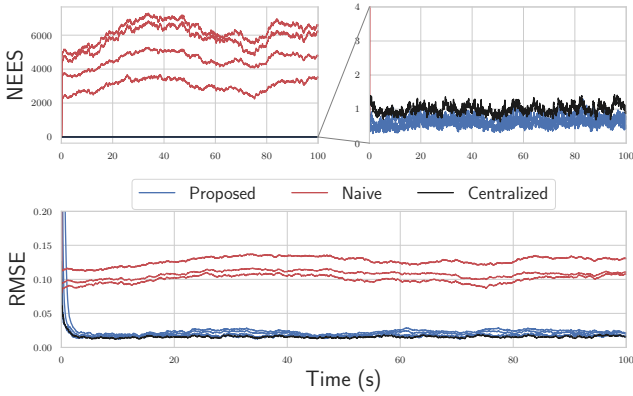


**Figure 3.** Results of 100 Monte Carlo trials for a four-robot version of the toy problem. The top two plots consist of a NEES plot, which is a measure of consistency. The bottom plot is the RMSE of the state. The proposed solution, which performs CI, remains statistically consistent and has reasonably low error in many cases.

for each pair  $(i, j) \in \mathcal{E}$ . Using MAP, the general state fusion problem is now

$$\hat{\mathcal{X}}_{1:N} = \operatorname{argmax}_{\mathcal{X}_{1:N}} p(\mathcal{X}_{1:N} | \mathbf{y}_{ij}), \quad \text{for all } (i, j) \in \mathcal{E}.$$

It is easier to instead consider a single pseudomeasurement at a time, such as, without loss of generality,  $\mathbf{y}_{12}$ . The posterior distribution given only  $\mathbf{y}_{12}$  is

$$\begin{aligned} p(\mathcal{X}_{1:N} | \mathbf{y}_{12}) &= \eta p(\mathbf{y}_{12} | \mathcal{X}_1, \mathcal{X}_2) p(\mathcal{X}_{1:N}) \\ &= \eta \mathcal{N}(\mathbf{c}_{12}(\mathcal{X}_1, \mathcal{X}_2), \Psi) \prod_{i=1}^N \mathcal{N}_L(\tilde{\mathcal{X}}_i, \tilde{\mathbf{P}}_i) \end{aligned} \quad (14)$$

where robot state priors have again been assumed to be independent, as a result of using covariance intersection. Due to this independence, the variables  $\mathcal{X}_{3:N}$  can be removed from the optimization problem since their optimal values are simply  $\hat{\mathcal{X}}_{3:N} = \tilde{\mathcal{X}}_{3:N}$  and have no effect on  $\mathcal{X}_1, \mathcal{X}_2$ . Minimizing the negative logarithm of (14), omitting terms involving  $\mathcal{X}_{3:N}$ , leads to a least-squares problem with error vector given by

$$\mathbf{e}(\mathcal{X}_1, \mathcal{X}_2) = \begin{bmatrix} \mathcal{X}_1 \ominus \tilde{\mathcal{X}}_1 \\ \mathcal{X}_2 \ominus \tilde{\mathcal{X}}_2 \\ -\mathbf{c}_{12}(\mathcal{X}_1, \mathcal{X}_2) \end{bmatrix},$$

and weight  $\mathbf{W} = \operatorname{diag}(\tilde{\mathbf{P}}_1^{-1}, \tilde{\mathbf{P}}_2^{-1}, \Psi^{-1})$ . Defining  $\mathbf{J}_i$  as the group Jacobian associated with  $G_i$ , as well as  $\mathbf{S}_i, \mathbf{S}_j$  being the jacobians of  $\mathbf{c}_{ij}$  with respect to  $\mathcal{X}_i, \mathcal{X}_j$ , respectively, the Jacobian of the error vector is

$$\mathbf{H} = \begin{bmatrix} \mathbf{J}_1^{-1} & \mathbf{0} \\ \mathbf{0} & \mathbf{J}_2^{-1} \\ -\mathbf{S}_1 & -\mathbf{S}_2 \end{bmatrix},$$

which is written without arguments  $(\mathcal{X}_1, \mathcal{X}_2)$  for brevity. The relevant terms of the Gauss-Newton system are

$$\begin{aligned} \mathbf{H}^T \mathbf{W} \mathbf{H} &= \\ & \begin{bmatrix} \mathbf{J}_1^{-T} \mathbf{P}_1^{-1} \mathbf{J}_1^{-1} + \mathbf{S}_1^T \Psi^{-1} \mathbf{S}_1 & \mathbf{S}_1^T \Psi^{-1} \mathbf{S}_2 \\ \mathbf{S}_2^T \Psi^{-1} \mathbf{S}_1 & \mathbf{J}_2^{-T} \mathbf{P}_2^{-1} \mathbf{J}_2^{-1} + \mathbf{S}_2^T \Psi^{-1} \mathbf{S}_2 \end{bmatrix}, \end{aligned}$$

$$\begin{aligned} \mathbf{H}^T \mathbf{W} \mathbf{e}(\mathcal{X}_1, \mathcal{X}_2) &= \\ & \begin{bmatrix} \mathbf{J}_1^{-T} \mathbf{P}_1^{-1} (\mathcal{X}_1 \ominus \tilde{\mathcal{X}}_1) - \mathbf{S}_1^T \Psi^{-1} \mathbf{c}_{12}(\mathcal{X}_1, \mathcal{X}_2) \\ \mathbf{J}_2^{-T} \mathbf{P}_2^{-1} (\mathcal{X}_2 \ominus \tilde{\mathcal{X}}_2) - \mathbf{S}_2^T \Psi^{-1} \mathbf{c}_{12}(\mathcal{X}_1, \mathcal{X}_2) \end{bmatrix}, \end{aligned}$$

which, by substantial manipulation with the SMW identities, can be used to analytically compute  $\delta \hat{\mathbf{x}} = (\mathbf{H}^T \mathbf{W} \mathbf{H})^{-1} \mathbf{H}^T \mathbf{W} \mathbf{e}(\hat{\mathcal{X}}_1, \hat{\mathcal{X}}_2)$ , producing on-manifold iterated-EKF-like expressions. The result is

$$\begin{aligned} \delta \hat{\mathbf{x}}_1 &= -\mathbf{J}_1 (\hat{\mathcal{X}}_1 \ominus \tilde{\mathcal{X}}_1) + \mathbf{K}_1 \mathbf{z}, \\ \delta \hat{\mathbf{x}}_2 &= -\mathbf{J}_2 (\hat{\mathcal{X}}_2 \ominus \tilde{\mathcal{X}}_2) + \mathbf{K}_2 \mathbf{z}, \\ \mathbf{K}_1 &= \mathbf{J}_1 \tilde{\mathbf{P}}_1 \mathbf{J}_1^T \mathbf{S}_1^T \mathbf{V}^{-1}, \\ \mathbf{K}_2 &= \mathbf{J}_2 \tilde{\mathbf{P}}_2 \mathbf{J}_2^T \mathbf{S}_2^T \mathbf{V}^{-1}, \\ \mathbf{z} &= -\mathbf{c}_{12}(\hat{\mathcal{X}}_1, \hat{\mathcal{X}}_2) + \mathbf{S}_1 \mathbf{J}_1 (\hat{\mathcal{X}}_1 \ominus \tilde{\mathcal{X}}_1) \\ &\quad + \mathbf{S}_2 \mathbf{J}_2 (\hat{\mathcal{X}}_2 \ominus \tilde{\mathcal{X}}_2), \\ \mathbf{V} &= \Psi + \mathbf{S}_1 \mathbf{J}_1 \tilde{\mathbf{P}}_1 \mathbf{J}_1^T \mathbf{S}_1^T + \mathbf{S}_2 \mathbf{J}_2 \tilde{\mathbf{P}}_2 \mathbf{J}_2^T \mathbf{S}_2^T, \end{aligned} \quad (15)$$

where iteration is done with  $\hat{\mathcal{X}}_i \leftarrow \hat{\mathcal{X}}_i \oplus \delta \hat{\mathbf{x}}_i$  after initialization with  $\hat{\mathcal{X}}_i \leftarrow \tilde{\mathcal{X}}_i$ . The marginal posterior covariances of Robots 1 and 2 are obtained from the corresponding diagonal blocks of  $(\mathbf{H}^T \mathbf{W} \mathbf{H})^{-1}$ , and can be shown to be

$$\begin{aligned} \hat{\mathbf{P}}_1 &= (\mathbf{1} - \mathbf{K}_1 \mathbf{S}_1) \mathbf{J}_1 \tilde{\mathbf{P}}_1 \mathbf{J}_1^T, \\ \hat{\mathbf{P}}_2 &= (\mathbf{1} - \mathbf{K}_2 \mathbf{S}_2) \mathbf{J}_2 \tilde{\mathbf{P}}_2 \mathbf{J}_2^T. \end{aligned} \quad (16)$$

The above fusion step introduces cross-correlations between the state estimates of  $\mathcal{X}_1$  and  $\mathcal{X}_2$ , and hence require a covariance intersection step

$$\hat{\mathbf{P}}_1 \leftarrow \frac{1}{w} \hat{\mathbf{P}}_1, \quad \hat{\mathbf{P}}_2 \leftarrow \frac{1}{1-w} \hat{\mathbf{P}}_2, \quad w \in (0, 1).$$

The next step is to make the approximation that  $p(\mathcal{X}_{1:N} | \mathbf{y}_{12}) \approx \prod_{i=1}^N \mathcal{N}_L(\hat{\mathcal{X}}_i, \hat{\mathbf{P}}_i)$ , and proceed with the fusion of a second pseudomeasurement, using  $p(\mathcal{X}_{1:N} | \mathbf{y}_{12}, \mathbf{y}_{13}) = \eta p(\mathbf{y}_{13} | \mathcal{X}_1, \mathcal{X}_3) p(\mathcal{X}_{1:N} | \mathbf{y}_{12})$ . This new posterior can again be approximated as Gaussian using the expressions in (15) and (16), and the process is repeated until all pseudomeasurements are incorporated. Algorithm 1 summarizes the general-purpose decentralized estimation algorithm from the point of view of an arbitrary robot. The algorithm is presented in a callback format, describing how the current state estimate is updated when various events occur.

**Algorithm 1** Decentralized estimation with no input sharing. For Robot  $i$  with process and measurement models given by (1), the following points break down how to compute the estimate when various events occur. Robot  $i$ 's estimate is initialized with  $\hat{\mathcal{X}}_{i_0}, \hat{\mathbf{P}}_{i_0}$ . The matrices  $\mathbf{F}_{i_k}, \mathbf{L}_{i_k}$  are the Jacobians of  $\mathbf{f}$  with respect to  $\mathcal{X}_{i_k}$  and  $\mathbf{w}_{i_k}$ , respectively. The matrix  $\mathbf{G}_{i_k}$  is the Jacobian of  $\mathbf{g}$ , and  $\mathbf{S}_{i_k}, \mathbf{S}_{j_k}$  are the Jacobians of  $\mathbf{c}_{ij}$  with respect to  $\mathcal{X}_{i_k}, \mathcal{X}_{j_k}$ , respectively.

- On the reception of an input measurement  $\mathbf{u}_{i_{k-1}}$ :

$$\begin{aligned}\hat{\mathcal{X}}_{i_k} &= \mathbf{f}(\hat{\mathcal{X}}_{i_{k-1}}, \mathbf{u}_{i_{k-1}}, \mathbf{0}), \\ \hat{\mathbf{P}}_{i_k} &= \mathbf{F}_{i_{k-1}} \hat{\mathbf{P}}_{i_{k-1}} \mathbf{F}_{i_{k-1}}^\top + \mathbf{L}_{i_{k-1}} \mathbf{Q}_{k-1} \mathbf{L}_{i_{k-1}}^\top.\end{aligned}$$

- On the reception of a local measurement  $\mathbf{y}_{i_k}$ :

$$\begin{aligned}\mathbf{K} &= \hat{\mathbf{P}}_{i_k} \mathbf{G}_{i_k}^\top (\mathbf{G}_{i_k} \hat{\mathbf{P}}_{i_k} \mathbf{G}_{i_k}^\top + \mathbf{R}_{i_k})^{-1}, \\ \delta \tilde{\mathbf{x}} &= \mathbf{K}(\mathbf{y}_{i_k} - \mathbf{g}(\hat{\mathcal{X}}_{i_k})), \\ \tilde{\mathcal{X}}_{i_k} &= \hat{\mathcal{X}}_{i_k} \oplus \delta \tilde{\mathbf{x}}, \\ \tilde{\mathbf{P}}_{i_k} &= (\mathbf{I} - \mathbf{K} \mathbf{G}_{i_k}) \hat{\mathbf{P}}_{i_k}.\end{aligned}$$

- On the reception of a neighbors' state estimate  $\tilde{\mathcal{X}}_{j_k}, \tilde{\mathbf{P}}_{j_k}$ :

$$\begin{aligned}\tilde{\mathbf{P}}_i &\leftarrow \frac{1}{w} \tilde{\mathbf{P}}_i, \quad \tilde{\mathbf{P}}_j \leftarrow \frac{1}{1-w} \tilde{\mathbf{P}}_j, \\ \mathbf{K} &= \tilde{\mathbf{P}}_{i_k} \mathbf{S}_{i_k}^\top (\Psi + \mathbf{S}_{i_k} \tilde{\mathbf{P}}_{i_k} \mathbf{S}_{i_k}^\top + \mathbf{S}_{j_k} \tilde{\mathbf{P}}_{j_k} \mathbf{S}_{j_k}^\top)^{-1}, \\ \delta \tilde{\mathbf{x}} &= -\mathbf{K}(\mathbf{c}_{ij}(\tilde{\mathcal{X}}_{i_k}, \tilde{\mathcal{X}}_{j_k})), \\ \hat{\mathcal{X}}_{i_k} &= \tilde{\mathcal{X}}_{i_k} \oplus \delta \tilde{\mathbf{x}}, \\ \hat{\mathbf{P}}_{i_k} &= (\mathbf{I} - \mathbf{K} \mathbf{G}_{i_k}) \tilde{\mathbf{P}}_{i_k},\end{aligned}$$

and optionally further iterate *both* robot estimates with (15), (16).

- At any time, send the current state estimate  $\hat{\mathcal{X}}_{j_k}, \hat{\mathbf{P}}_{j_k}$  to neighbors.

## 5.1 An Observability Test

In a decentralized state estimation context, the full system state is the concatenation of all the robots' states. Hence, observability of this system refers to the ability to recover the state trajectory of *each* robot given the inputs and measurements of *all* robots. An observability test for decentralized estimators should therefore take into account all the local measurements collected by each robot *and* what information is communicated between them. Consider again the simple toy problem described in Section 4, but with neither robot collecting absolute position measurements, thus making both robot's states unobservable. Performing a standard observability test for an individual robot, treating the other robot's estimate as a "measurement", will falsely conclude that the system is observable. On the other hand, the upcoming observability test will correctly indicate that there is an unobservable degree of freedom in the joint system state, through rank deficiency of an observability matrix.

The pseudomeasurements encode the communication structure between the robots. An advantage of this proposed approach is that it allows the straightforward application

of common observability tests to the entire team of robots, viewed as a single system. A *local* observability test can be formed by considering the MAP problem on an entire trajectory simultaneously, but without prior information on the initial state (Psiaki (2013)). Let the bolded  $\mathcal{X}_k = (\mathcal{X}_{1_k}, \dots, \mathcal{X}_{N_k})$  denote the state of all robots at time step  $k$ ,  $\mathbf{y}_k = [\mathbf{y}_{1_k}^\top \dots \mathbf{y}_{N_k}^\top]^\top$  denote a stacked vector containing all the robots' local measurements at time step  $k$ . Let  $\psi_k = [\dots \mathbf{y}_{ij}^\top \dots]^\top$ ,  $(i, j) \in \mathcal{E}$  denote the stacked pseudomeasurements between all robots at time step  $k$ . The MAP problem is

$$\hat{\mathcal{X}}_{0:K} = \underset{\mathcal{X}_{0:K}}{\operatorname{argmax}} p(\mathcal{X}_{0:K} | \mathbf{y}_{0:K}, \psi_{0:K})$$

with

$$p(\mathcal{X}_{0:K} | \mathbf{y}_{0:K}, \psi_{0:K}) = \eta \prod_{k=0}^K p(\mathbf{y}_0 | \mathcal{X}_0) p(\psi_0 | \mathcal{X}_0) \prod_{k=1}^K p(\mathcal{X}_k | \mathcal{X}_{k-1}),$$

leading to a nonlinear least squares problem with weight  $\mathbf{W}$  and error vector

$$\begin{aligned}\mathbf{e}(\mathcal{X}_{0:K}) &= [\dots \mathbf{e}_{u,k} \dots \mathbf{e}_{y,k} \dots \mathbf{e}_{\psi,k} \dots]^\top, \\ \mathbf{e}_{u,k} &= [\dots (\mathcal{X}_{i_k} \ominus \mathbf{f}(\mathcal{X}_{i_{k-1}}, \mathbf{u}_{i_{k-1}}))^\top \dots], \\ \mathbf{e}_{y,k} &= [\dots (\mathbf{y}_{i_k} - \mathbf{g}(\mathcal{X}_{i_k}))^\top \dots], \quad i = 1, \dots, N, \\ \mathbf{e}_{\psi,k} &= [\dots -\mathbf{c}_{ij}(\mathcal{X}_{i_k}, \mathcal{X}_{j_k})^\top \dots], \quad (i, j) \in \mathcal{E}.\end{aligned}$$

The error Jacobian is

$$\mathbf{H} = \begin{bmatrix} -\mathbf{F}_0 & \mathbf{1} & & & \\ & \ddots & \ddots & & \\ & & -\mathbf{F}_{K-1} & \mathbf{1} & \\ -\mathbf{G}_0 & & -\mathbf{G}_1 & & \\ & & & \ddots & \\ -\Phi_0 & & & & -\mathbf{G}_K \\ & -\Phi_1 & & & \\ & & \ddots & & \\ & & & & -\Phi_K \end{bmatrix},$$

$$\begin{aligned}\mathbf{F}_k &= \operatorname{diag} \left( \dots, \frac{D\mathbf{f}(\mathcal{X}_{i_k}, \mathbf{u}_{i_k})}{D\mathcal{X}_{i_k}}, \dots \right), \\ \mathbf{G}_k &= \operatorname{diag} \left( \dots, \frac{D\mathbf{g}(\mathcal{X}_{i_k})}{D\mathcal{X}_{i_k}}, \dots \right), \quad i = 1, \dots, N, \\ \Phi_k &= -\frac{D\mathbf{e}_{\psi,k}(\mathcal{X}_k)}{D\mathcal{X}_k},\end{aligned}$$

with all undisplayed entries in  $\mathbf{H}$  equal to zero. For the solution to the MAP problem to be unique, then to first order,  $(\mathbf{H}^\top \mathbf{W} \mathbf{H})$  must be invertible, and thus full rank. Fortunately,  $\mathbf{W}$  is always positive definite regardless of any cross-correlations that would add off-diagonal entries. Hence,  $\operatorname{rank}(\mathbf{H}^\top \mathbf{W} \mathbf{H}) = \operatorname{rank}(\mathbf{H})$ , and it is thus required that  $\mathbf{H}$  be full column rank. This implies that the proposed observability test is unaffected by the approximation induced

by CI, or any cross-correlation terms that may or may not be successfully tracked. In a similar way to (Barfoot 2023, Ch 3.1.4), it can be shown that by performing a variety of elementary row/column operations, the rank of  $\mathbf{H}$  is equivalent to the rank of

$$\mathcal{O} = \begin{bmatrix} \mathbf{M}_0 \\ \mathbf{M}_1 \mathbf{F}_0 \\ \vdots \\ \mathbf{M}_K \mathbf{F}_{K-1} \dots \mathbf{F}_0 \end{bmatrix}, \quad \mathbf{M}_k = \begin{bmatrix} \mathbf{G}_k \\ \Phi_k \end{bmatrix}.$$

Hence, if  $\mathcal{O}$  has maximum rank, the solution to the MAP problem is locally unique, and the system is said to be observable. Note that this test easily allows for time-varying graphs, which would yield a different  $\Phi_k$  for each time step  $k$ .

## 6 Efficient Odometry Sharing using Preintegration

Many problems, especially those where robots estimate their neighbors' positions, will require robots to have access to their neighbors' process-model input values  $\mathbf{u}$ . Until now, it has been assumed that all robots have unrestricted access to each other's inputs. In robot state estimation applications, the input is often the odometry measurements, such as wheel encoder or IMU measurements. These can occur at frequencies of 100 - 1000 Hz, and can therefore be infeasible to share in real time, especially if multiple robots are to simultaneously share measurements at high frequency. This could quickly reach a bandwidth limit on the common communication channel, such as ultra-wideband radio.

The proposed solution to this problem is to use *preintegration*. That is, robots will instead share preintegrated input measurements over an arbitrary duration of time instead of individual input measurements. Specifically, consider the following generic process model

$$\mathcal{X}_k = \mathbf{f}(\mathcal{X}_{k-1}, \mathbf{u}_{k-1}, \mathbf{w}_{k-1}).$$

The action of preintegration is to directly iterate this process model by repeated compositions in order to, after algebraic manipulation, generate a new *preintegrated process model*  $\mathbf{f}_{pq}$  that relates two states at arbitrary time steps  $k = p$  and  $k = q$ . That is,

$$\begin{aligned} \mathcal{X}_{p+1} &= \mathbf{f}(\mathcal{X}_p, \mathbf{u}_p, \mathbf{w}_p), \\ \mathcal{X}_{p+2} &= \mathbf{f}(\mathbf{f}(\mathcal{X}_p, \mathbf{u}_p, \mathbf{w}_p), \mathbf{u}_{p+1}, \mathbf{w}_{p+1}), \\ &\vdots \\ \mathcal{X}_q &= \mathbf{f}(\mathbf{f}(\dots \mathbf{f}(\mathcal{X}_p, \mathbf{u}_p, \mathbf{w}_p) \dots), \mathbf{u}_{q-1}, \mathbf{w}_{q-1}) \\ &\triangleq \mathbf{f}_{pq}(\mathcal{X}_p, \Delta\mathcal{X}_{pq}) \oplus \mathbf{w}_{pq}, \end{aligned}$$

where  $\Delta\mathcal{X}_{pq}$  is the *relative motion increment* (RMI), which in general may also belong to a Lie group, and  $\mathbf{w}_{pq} \sim \mathcal{N}(\mathbf{0}, \mathbf{Q}_{pq})$  is the *preintegrated noise*. The advantages of preintegration will stem from the careful choice of RMI definition, which is ideally done such that the RMI has the following properties.

1. The RMI is determined from the input measurements exclusively, and is independent of the state estimate:

$$\Delta\mathcal{X}_{pq} = \Delta\mathcal{X}_{pq}(\mathbf{u}_{p:q-1}).$$

2. Far fewer numbers are required to represent the RMI than the  $(q - p)$  raw measurements that occurred during the preintegration interval:

$$\dim(\Delta\mathcal{X}_{pq}) \ll (q - p) \dim(\mathbf{u}_k).$$

If the above points are true, communicating  $\Delta\mathcal{X}_{pq}, \mathbf{Q}_{pq}$  instead of  $\mathbf{u}_{p:q-1}$  will not only reduce the communication cost, but will also result in a fixed message size and ability to directly predict the state forward over a long duration of time, instead of sequentially processing the measurements. It turns out that many common process models in robotics are amenable to preintegration, and furthermore are typically extremely fast to preintegrate incrementally as input measurements are obtained. That is, there exists a function  $\text{INCREMENT}(\cdot)$  such that

$$\Delta\mathcal{X}_{pq}, \mathbf{Q}_{pq} = \text{INCREMENT}(\Delta\mathcal{X}_{p:q-1}, \mathbf{Q}_{p:q-1}, \mathbf{u}_{q-1}).$$

A few examples now follow, which describe concrete implementations of  $\Delta\mathcal{X}_{pq}, \mathbf{f}_{pq}(\cdot)$ , and  $\text{INCREMENT}(\cdot)$ .

**Example 1.** Linear preintegration. *The linear process model*

$$\mathbf{x}_k = \mathbf{F}_{k-1} \mathbf{x}_{k-1} + \mathbf{L}_{k-1} \mathbf{u}_{k-1}$$

can be directly iterated to yield

$$\begin{aligned} \mathbf{x}_q &= \left( \prod_{k=p}^{q-1} \mathbf{F}_k \right) \mathbf{x}_p + \sum_{k=p}^{q-1} \left( \prod_{\ell=k+1}^{q-1} \mathbf{F}_\ell \right) \mathbf{L}_k \mathbf{u}_k \\ &\triangleq \mathbf{F}_{pq} \mathbf{x}_p + \Delta\mathbf{x}_{pq}, \end{aligned} \quad (17)$$

where (17) defined  $\mathbf{f}(\cdot)$ . Assuming that noise enters the model additively through the input  $\mathbf{u}_k = \bar{\mathbf{u}}_k + \mathbf{w}_k$ , where  $\mathbf{w}_k \sim \mathcal{N}(\mathbf{0}, \mathbf{Q}_k)$ , (17) becomes  $\mathbf{x}_j = \mathbf{F}_{pq} \mathbf{x}_i + \Delta\bar{\mathbf{x}}_{pq} + \mathbf{w}_{pq}$  where

$$\begin{aligned} \mathbf{w}_{pq} &\triangleq \sum_{k=p}^{q-1} \left( \prod_{\ell=k+1}^{q-1} \mathbf{F}_\ell \right) \mathbf{L}_k \mathbf{w}_k, \\ &= \mathbf{F}_{q-1} \mathbf{w}_{pq-1} + \mathbf{L}_{q-1} \mathbf{w}_{q-1}. \end{aligned}$$

The RMI  $\Delta\mathbf{x}_{pq}$  and corresponding covariance are therefore built incrementally with

$$\begin{aligned} \Delta\mathbf{x}_{pq} &= \mathbf{F}_{q-1} \Delta\mathbf{x}_{pq-1} + \mathbf{L}_{q-1} \mathbf{u}_{q-1}, \\ \mathbf{Q}_{pq} &= \mathbf{F}_{q-1} \mathbf{Q}_{pq-1} \mathbf{F}_{q-1}^\top + \mathbf{L}_{q-1} \mathbf{Q}_{q-1} \mathbf{L}_{q-1}^\top, \end{aligned}$$

which together define the  $\text{INCREMENT}(\cdot)$  function.

**Example 2.** Wheel odometry preintegration on  $SE(2)$ . Given a robot pose  $\mathbf{T} \in SE(2)$ , the wheel odometry process model is given by

$$\mathbf{T}_k = \mathbf{T}_{k-1} \text{Exp}(\Delta\mathbf{t}\mathbf{u}_{k-1}),$$

where  $\mathbf{u} = [\omega \ v \ 0]^\top$ ,  $\omega$  is the robot's heading rate-of-change, and  $v$  is its forward velocity in its own body frame. Direct iteration yields the preintegrated process model  $\mathbf{f}_{pq}(\cdot)$  given by

$$\mathbf{T}_q = \mathbf{T}_p \underbrace{\prod_{k=p}^{q-1} \text{Exp}(\Delta\mathbf{t}\mathbf{u}_k)}_{\triangleq \Delta\mathbf{T}_{pq}}.$$



Noise  $\mathbf{w}_k \sim \mathcal{N}(\mathbf{0}, \mathbf{Q}_k)$  is again assumed to enter additively through the input, and a series of first-order approximations lead to

$$\begin{aligned} \Delta \mathbf{T}_{pq} &= \prod_{k=p}^{q-1} \text{Exp}(\Delta t(\bar{\mathbf{u}}_k + \mathbf{w}_k)) \\ &\approx \prod_{k=p}^{q-1} \text{Exp}(\Delta t\bar{\mathbf{u}}_k) \text{Exp}(\Delta t\mathbf{J}_k \mathbf{w}_k) \\ &\approx \underbrace{\Delta \bar{\mathbf{T}}_{pq} \prod_{k=p}^{q-1} \text{Exp}(\Delta t \text{Ad}(\Delta \mathbf{T}_{k+1}^{-1}) \mathbf{J}_k \mathbf{w}_k)}_{\text{Exp}(\mathbf{w}_{pq})}, \end{aligned}$$

where  $\mathbf{J}_k \triangleq \mathbf{J}(\Delta t\bar{\mathbf{u}}_k)$  is the right Jacobian of  $SE(2)$ . Having identified an expression for  $\text{Exp}(\mathbf{w}_{pq})$ , under the assumption that  $\mathbf{w}_{pq}$  is small,

$$\begin{aligned} \mathbf{w}_{pq} &\approx \sum_{k=p}^{q-1} \Delta t \text{Ad}(\Delta \mathbf{T}_{k+1}^{-1}) \mathbf{J}_k \mathbf{w}_k \\ &= \sum_{k=p}^{q-2} \Delta t \text{Ad}(\Delta \mathbf{T}_{k+1}^{-1}) \mathbf{J}_k \mathbf{w}_k \\ &\quad + \Delta t \underbrace{\text{Ad}(\Delta \mathbf{T}_{qq}^{-1}) \mathbf{J}_{q-1} \mathbf{w}_{q-1}}_{\mathbf{1}} \\ &= \underbrace{\text{Ad}(\Delta \mathbf{T}_{q-1}^{-1}) \mathbf{w}_{pq-1}}_{\triangleq \mathbf{F}_{q-1}} + \underbrace{\Delta t \mathbf{J}_{q-1} \mathbf{w}_{q-1}}_{\triangleq \mathbf{L}_{q-1}}, \end{aligned}$$

and the defining operations of the  $\text{INCREMENT}(\cdot)$  function follow,

$$\begin{aligned} \Delta \mathbf{T}_{pq} &= \Delta \mathbf{T}_{pq-1} \text{Exp}(\Delta t\mathbf{u}_k), \\ \mathbf{Q}_{pq} &= \mathbf{F}_{q-1} \mathbf{Q}_{pq-1} \mathbf{F}_{q-1}^T + \mathbf{L}_{q-1} \mathbf{Q}_{q-1} \mathbf{L}_{q-1}^T. \end{aligned}$$

**Example 3.** IMU preintegration. Being the most well-known usage of preintegration, a complete reference for IMU preintegration on the  $SO(3) \times \mathbb{R}^3 \times \mathbb{R}^3$  manifold can be obtained from [Forster et al. \(2017\)](#), and alternatively for the  $SE_2(3)$  group from [Brossard et al. \(2022\)](#); [Barfoot \(2023\)](#). Either approach can be used with the framework in this paper. However in Section 8 of this paper,  $\mathbf{T}_{wi} \in SE_2(3)$  matrices are used to represent the extended pose of Robot  $i$  relative to an inertial world frame  $w$ . Following [Shalaby et al. \(2023\)](#) and [Brossard et al. \(2022\)](#), it can be shown that the discrete-time IMU kinematic equations can be written in the form

$$\mathbf{T}_{wi_k} = \mathbf{G}_{k-1} \mathbf{T}_{wi_{k-1}} \mathbf{U}_{k-1}, \quad (18)$$

where

$$\begin{aligned} \mathbf{T}_{wi_k} &= \begin{bmatrix} \mathbf{C} & \mathbf{v} & \mathbf{r} \\ \mathbf{0} & 1 & 0 \\ \mathbf{0} & 0 & 1 \end{bmatrix} \\ \mathbf{G}_{k-1} &= \begin{bmatrix} \mathbf{1} & \Delta t \mathbf{g} & -\frac{\Delta t^2}{2} \mathbf{g} \\ 0 & 1 & -\Delta t \\ 0 & 0 & 1 \end{bmatrix} \\ \mathbf{U}_{k-1} &= \begin{bmatrix} \exp(\Delta t \boldsymbol{\omega}^\wedge) & \Delta t \mathbf{J}(\Delta t \boldsymbol{\omega}) \mathbf{a} & \frac{\Delta t^2}{2} \mathbf{N}(\Delta t \boldsymbol{\omega}) \mathbf{a} \\ 0 & 1 & \Delta t \\ 0 & 0 & 1 \end{bmatrix} \\ \mathbf{N}(\boldsymbol{\phi}) &= \mathbf{z} \mathbf{z}^\top + 2 \left( \frac{1}{\phi} - \frac{\sin \phi}{\phi^2} \right) \mathbf{z}^\wedge + 2 \frac{\cos \phi - 1}{\phi^2} \mathbf{z}^\wedge \mathbf{z}^\wedge \\ \phi &= \|\boldsymbol{\phi}\|, \quad \mathbf{z} = \boldsymbol{\phi} / \phi, \end{aligned}$$

and  $\mathbf{C} \in SO(3)$ ,  $\mathbf{v}$ ,  $\mathbf{r}$  respectively represent attitude, velocity, position relative to frame  $w$ ,  $\boldsymbol{\omega}$  is the IMU's unbiased gyro measurement,  $\mathbf{a}$  is the IMU's unbiased accelerometer measurement,  $\mathbf{g}$  is the gravity vector resolved in frame  $w$ , and  $\mathbf{J}(\boldsymbol{\phi})$  is the left Jacobian of  $SO(3)$ . Preintegration of these kinematics is easily achieved by direct iteration with

$$\begin{aligned} \mathbf{T}_{wi_q} &= \left( \prod_{k=p}^{q-1} \mathbf{G}_{k-1} \right) \mathbf{T}_{wi_p} \left( \prod_{k=p}^{q-1} \mathbf{U}_{k-1} \right) \\ &\triangleq \Delta \mathbf{G}_{pq} \mathbf{T}_{wi_p} \Delta \mathbf{U}_{pq}, \end{aligned}$$

where  $\Delta \mathbf{U}_{pq}$  is the RMI, and the noise statistics can be propagated through this preintegration process by a standard linearization procedure. [Shalaby et al. \(2023\)](#) present the details of the noise propagation, as well as how to adapt this formulation for relative poses.

## 6.1 Multi-robot preintegration

In the context of multi-robot estimation problems, an individual robot's process model may involve the input values of many neighboring robots. To reflect this, rewrite the process model for Robot  $i$  as

$$\mathcal{X}_{i_k} = \mathbf{f}(\mathcal{X}_{i_{k-1}}, \mathbf{u}_{i_{k-1}}, \mathbf{u}_{j_{k-1}}), \quad j \in \mathcal{N}_i, \quad (19)$$

where  $\mathbf{u}_{i_k}$  denotes an input measured by Robot  $i$  and  $\mathcal{N}_i$  denotes the set of neighbor IDs of Robot  $i$ . The preintegrated process model would now be written as

$$\mathcal{X}_{i_q} = \mathbf{f}_{pq}(\mathcal{X}_{i_p}, \Delta \mathcal{X}_{i_{pq}}, \Delta \mathcal{X}_{j_{pq}}), \quad j \in \mathcal{N}_i, \quad (20)$$

where  $\Delta \mathcal{X}_{i_{pq}}$  denotes an RMI calculated from the input measurements of Robot  $i$ .

A complication is that the RMIs from neighboring Robots  $\Delta \mathcal{X}_{j_{pq}}$  are only available asynchronously, meaning it is not always possible to evaluate (20) directly. To deal with this, assume that the preintegrated process model  $\mathbf{f}_{pq}$  is compatible with

$$\begin{aligned} \mathfrak{X}_{i_{k-1}} &= \mathbf{f}(\mathcal{X}_{i_{k-2}}, \mathbf{u}_{i_{k-2}}, \mathbf{0}), \\ \mathfrak{X}_{i_k} &= \mathbf{f}(\mathfrak{X}_{i_{k-1}}, \mathbf{u}_{i_{k-1}}, \mathbf{0}), \\ \mathcal{X}_{i_k} &= \mathbf{f}_{pq}(\mathfrak{X}_{i_k}, \mathcal{I}, \Delta \mathcal{X}_{j_{pq}}), \end{aligned}$$

where  $\mathcal{I}$  is the identity element. The variable  $\mathfrak{X}_{i_k}$  represents an intermediate, non-physical state that is

continuously propagated using the process model without input information from neighboring robots. Sometime later, at arbitrary time step  $k = q$ , the RMI from a neighboring robot  $\Delta\mathcal{X}_{j_{pq}}$  is received and this intermediate state  $\tilde{\mathcal{X}}_{i_q}$  is propagated back into a physically meaningful quantity  $\mathcal{X}_{i_q}$ . A concrete example of this asynchronous intermediate state updating is shown in Section 7, and a summary is shown in Algorithm 2.

---

**Algorithm 2** Decentralized estimation with preintegration.

The setup is identical to Algorithm 1, except that the process model requires input information from neighboring robots as in (19), (20).

- On the reception of a local input measurement  $\mathbf{u}_{i_{k-1}}$ :

$$\begin{aligned}\tilde{\mathcal{X}}_{i_k} &= \mathbf{f}(\hat{\mathcal{X}}_{i_{k-1}}, \mathbf{u}_{i_{k-1}}, \mathbf{0}) \\ \tilde{\mathfrak{P}}_{i_k} &= \mathbf{F}_{i_{k-1}} \hat{\mathbf{P}}_{i_{k-1}} \mathbf{F}_{i_{k-1}}^\top + \mathbf{L}_{i_{k-1}} \mathbf{Q}_{k-1} \mathbf{L}_{i_{k-1}}^\top,\end{aligned}$$

and increment Robot  $i$ 's own RMI,

$$\Delta\mathcal{X}_{i_{pk}}, \mathbf{Q}_{i_{pk}} = \text{INCREMENT}(\Delta\mathcal{X}_{i_{pk-1}}, \mathbf{Q}_{i_{pk-1}}, \mathbf{u}_{i_{k-1}}).$$

- Whenever required, send  $\Delta\mathcal{X}_{i_{pq}}, \mathbf{Q}_{i_{pq}}$  to neighbors.
- On the reception of a neighboring robot's RMI and covariance  $\Delta\mathcal{X}_{j_{pq}}, \mathbf{Q}_{j_{pq}}$ ,

$$\begin{aligned}\mathcal{X}_{i_q} &= \mathbf{f}_{pq}(\tilde{\mathcal{X}}_{i_q}, \mathcal{I}, \Delta\mathcal{X}_{j_{pq}}), \\ \mathbf{F}_{pq} &= \left. \frac{D\mathbf{f}_{pq}(\tilde{\mathcal{X}}, \mathcal{I}, \Delta\mathcal{X}_{j_{pq}})}{D\tilde{\mathcal{X}}} \right|_{\tilde{\mathcal{X}}_{i_q}}, \\ \tilde{\mathbf{P}}_{i_q} &= \mathbf{F}_{pq} \tilde{\mathfrak{P}}_{i_{k-1}} \mathbf{F}_{pq}^\top + \mathbf{Q}_{j_{pq}}.\end{aligned}$$

- On the reception of a local measurement  $\mathbf{y}_{i_k}$ , proceed as per Algorithm 1.
  - On the reception of a neighbors' state estimate  $\tilde{\mathcal{X}}_j, \tilde{\mathbf{P}}_j$ , proceed as per Algorithm 1.
  - At any time, send the current state estimate  $\tilde{\mathcal{X}}_{j_k}, \tilde{\mathbf{P}}_{j_k}$  to neighbors.
- 

## 6.2 Estimating Input Biases

For some problems, it may be desired to estimate an input bias  $\mathbf{b}$  as part of the overall state  $\mathcal{X}$ , a setup commonly occurring in inertial navigation where accelerometer and rate gyro biases are estimated. The difficulty lies in the frequent inability to express RMIs independently of the bias values, thus leaving RMIs in the form of

$$\Delta\mathcal{X}_{pq}(\mathbf{u}_{p:q-1}, \mathbf{b}_{p:q-1}).$$

In the context of the multi-robot estimation scheme shown in Algorithm 2, computing RMIs this way causes inconsistency in the filter, since the RMIs are now correlated with the robot states. Accounting for this would require maintaining the cross-correlation between a robot's state and their neighbors' biases.

A simpler alternate solution is to have robots estimate their neighbors' input biases in addition to their own. This requires to exploit the fact that biases are usually modelled to follow a random walk, and therefore have a constant mean in the absence of any correcting information. This motivates the

approximation  $\mathbf{b}_p \approx \mathbf{b}_{p+1} \approx \dots \approx \mathbf{b}_q$  and hence

$$\Delta\mathcal{X}_{pq}(\mathbf{u}_{p:q-1}, \mathbf{b}_{p:q-1}) \approx \Delta\mathcal{X}_{pq}(\mathbf{u}_{p:q-1}, \mathbf{b}_q).$$

When robots receive input measurements, they increment their RMIs with raw (biased) inputs to produce  $\Delta\mathcal{X}_{pq}(\mathbf{u}_{p:q-1}, \mathbf{0})$ . At an appropriate time, they share their current biased RMIs, which is corrected for bias by the receiving robot using the first-order approximation

$$\begin{aligned}\Delta\mathcal{X}_{pq}(\mathbf{u}_{p:q-1}, \mathbf{b}_q) &\approx \Delta\mathcal{X}_{pq}(\mathbf{u}_{p:q-1}, \mathbf{0}) \oplus \mathbf{B}_{pq} \mathbf{b}_q, \quad (21) \\ \mathbf{B}_{pq} &\triangleq \frac{D}{D\mathbf{b}_q} \left( \Delta\mathcal{X}_{pq}(\mathbf{u}_{p:q-1}, \mathbf{b}_q) \right),\end{aligned}$$

where  $\mathbf{B}_{pq}$  is defined as the bias jacobian. Equation (21) is an approximation that contributes unmodelled errors to the estimation problem, relying on an assumption that  $\mathbf{b}_q$  is small. This can be enabled by a proper offline calibration procedure that removes any large bias, and only small deviations from this are estimated online. Such a procedure is used for the quadcopter problem in Section 8, where good, consistent estimation results are still obtained despite the approximation in (21).

## 6.3 Autoencoding Covariance Matrices

As shown in Algorithm 2, predicting state estimates that are a function of neighbor inputs requires the RMI  $\Delta\mathcal{X}_{pq}$  along with a corresponding covariance  $\mathbf{Q}_{pq}$ . As is, these two quantities must be shared between robots. This section proposes an optional method that further reduces communication costs by eliminating the requirement to share the preintegrated covariance  $\mathbf{Q}_{pq}$ .

The key insight is that  $\Delta\mathcal{X}_{pq}(\mathbf{u}_{p:q-1})$  and  $\mathbf{Q}_{pq}(\mathbf{u}_{p:q-1})$  are both calculated from the same input values  $\mathbf{u}_{p:q-1}$ . Hence, if an alternate mapping  $\mathbf{Q}_{pq} = \mathbf{h}(\Delta\mathcal{X}_{pq})$  existed, then it would be sufficient to share  $\Delta\mathcal{X}_{pq}$  only, and the receiving robot could infer  $\mathbf{Q}_{pq}$  directly from the RMI. In the absence of analytic expressions for  $\mathbf{h}(\cdot)$ , this paper approximates the function with a neural network, trained on purely synthetic RMI-covariance pairs. An additional complication is that such a function  $\mathbf{h}(\cdot)$  may not always exist since an RMI can correspond to many possible covariances depending on the input values. In this case  $\mathbf{h}(\cdot)$  is not a true function since it is one-to-many, and its definition is modified to also accept a low-dimensional *encoding*  $\mathbf{e}(\mathbf{Q}_{pq})$ , leading to  $\mathbf{Q}_{pq} = \mathbf{h}(\Delta\mathcal{X}_{pq}, \mathbf{e}(\mathbf{Q}_{pq}))$ . This leads to an architecture here referred to as *mean-assisted autoencoding*, depicted in Figure 4.

The flattened lower-triangular half of  $\mathbf{Q}_{pq}$  is given to a simple fully-connected *encoder* network with GELU activation functions and a single hidden layer. The output of

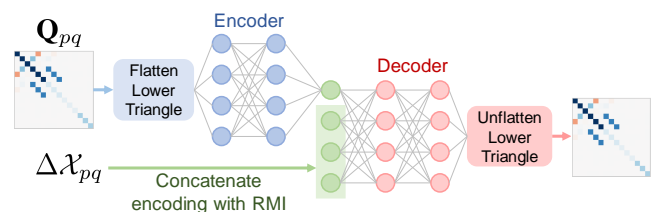


**Figure 4.** Concept diagram of mean-assisted autoencoder.

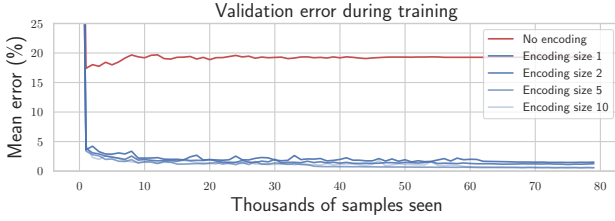


**Figure 5.** Mean percentage reconstruction error throughout training for various encoding sizes including no encoding. A single encoding number is sufficient to achieve less than 1% reconstruction error on average.

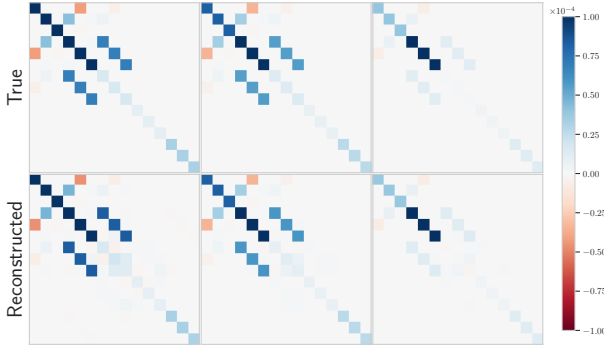


**Figure 6.** Visualization of preintegrated IMU noise covariance matrices along with reconstruction using mean-assisted autoencoding.

this network is the encoding, which can be as small as one or two numbers. This encoding is then concatenated with a parameterization of the RMI  $\Delta\mathcal{X}_{pq}$  and fed to a similar *decoder* network. The decoder network outputs the flattened lower-triangular half of a reconstructed covariance matrix denoted  $\hat{\mathbf{Q}}_{pq}$ . For training, the loss function simply uses the Frobenius norm,

$$\mathcal{L}(\mathbf{Q}_{pq}, \hat{\mathbf{Q}}_{pq}) = \|\mathbf{Q}_{pq} - \hat{\mathbf{Q}}_{pq}\|_F.$$

Figure 5 shows the training convergence history for various encoding sizes, applied to IMU preintegration. The Adam optimizer is chosen with an initial learning rate of  $10^{-3}$  that is scheduled to decrease once the loss plateaus. The encoder/decoder networks have hidden layers with 256 neurons, and the training process takes just a few minutes on a laptop CPU to achieve less than 1% average reconstruction error on a validation dataset from experimental data. The training data is purely synthetic, where RMIs are constructed from a random amount of random IMU measurements, with values covering the realistic range of real IMU measurements. Since the length of the dataset is infinite, the risk of overfitting is completely eliminated. A visualization of the reconstructed covariance matrices can be seen in Figure 5, using an encoding size of only 1 number. Section 8 will employ this method “in the loop” for a real quadcopter problem. It will be shown that the reconstruction error is so small that the impact on the estimation results are negligible.

Concretely, using IMU preintegration as an example, the RMI itself must be communicated, which requires 10 floating-point numbers. However, the covariance matrix is  $15 \times 15$ , which would require communication of an additional 120 floating-point numbers to represent one of

its triangular halves. With the proposed autoencoder, these 120 numbers are replaced with an encoding consisting of *one* number, thus dramatically reducing the communication cost.

## 7 Simulation with Ground Robots

The proposed algorithm is tested in a simulation with ground robots, shown in the center of Figure 1. Each robot estimates their own pose and their neighbors’ poses relative to a world frame. Denoting the pose of Robot  $i$  relative to the world frame  $w$  as  $\mathbf{T}_{wi} \in SE(2)$ , the state of an arbitrary robot is given by

$$\mathcal{X}_{i_k} = \left( \mathbf{T}_{wi_k}^{[i]}, \mathbf{T}_{wj_k}^{[j]}, \dots \right), \quad j \in \mathcal{N}_i,$$

where, again, the  $(\cdot)^{[i]}$  superscript indicates Robot  $i$ ’s estimate or “instance” of that physical quantity. Each robot collects wheel odometry at 100 Hz, providing  $\mathbf{u}_{i_k} = [\omega_{i_k} \ v_{i_k} \ 0]^T$  as input measurements, where  $\omega_{i_k}$  is Robot  $i$ ’s angular velocity and  $v_{i_k}$  is its forward velocity in its own body frame. The pose kinematics for any single robot along with its preintegration are shown in Example 2. When Robot  $i$  receives an input measurement, it updates the part of its state corresponding to its own pose to create

$$\tilde{\mathcal{X}}_{i_k} = \left( \mathbf{T}_{iw_{k-1}}^{[i]} \text{Exp}(\Delta t \mathbf{u}_{i_{k-1}}), \mathbf{T}_{wj_{k-1}}^{[j]}, \dots \right).$$

The neighbor poses  $\mathbf{T}_{wj_{k-1}}$  are now out of date, as neighboring odometry information is not yet accessible to Robot  $i$ , and this partially out-of-date state is non-physical and given the symbol  $\tilde{\mathcal{X}}_{i_k}$ . When a neighbor’s RMI  $\Delta\mathbf{T}_{j_{pq}}$  is received at some later time step  $k = q$ , the state is updated with

$$\mathcal{X}_{i_q} = \left( \mathbf{T}_{iw_q}^{[i]}, \mathbf{T}_{wj_p}^{[j]} \Delta\mathbf{T}_{j_{pq}}, \dots \right)$$

where  $p$  represents the time step index of the last time a neighbor RMI was received.

Each robot also collects range measurements to its neighbors at 10 Hz, and only two robots collect relative position measurements to known landmarks at 10 Hz. At an arbitrary separate frequency, each robot sends its current state and covariance to its neighbors, allowing the neighbors to compute pseudomeasurements of the form

$$\mathbf{c}_{ij}(\mathcal{X}_i, \mathcal{X}_j) = \begin{bmatrix} \text{Log} \left( \mathbf{T}_{wi}^{[i]-1} \mathbf{T}_{wj}^{[j]} \right) \\ \text{Log} \left( \mathbf{T}_{wj}^{[j]-1} \mathbf{T}_{wi}^{[i]} \right) \\ \text{Log} \left( \mathbf{T}_{wl}^{[l]-1} \mathbf{T}_{wl}^{[l]} \right) \\ \vdots \end{bmatrix}, \quad \ell \in \mathcal{N}_i \cap \mathcal{N}_j.$$

A simulation is performed with 4 robots each executing Algorithm 2, with root-mean-squared error (RMSE) and normalized estimation error squared (NEES) plots shown in Figure 7 and 8, respectively. The results show that all four robots’ estimation errors successfully stabilize and remain low, despite only two robots having sufficient sensors to make their states observable. The decentralized solution is slightly underconfident, but this is preferred compared to overconfidence. If state fusion is done at a sufficiently high frequency, performance is even comparable to the centralized estimator.

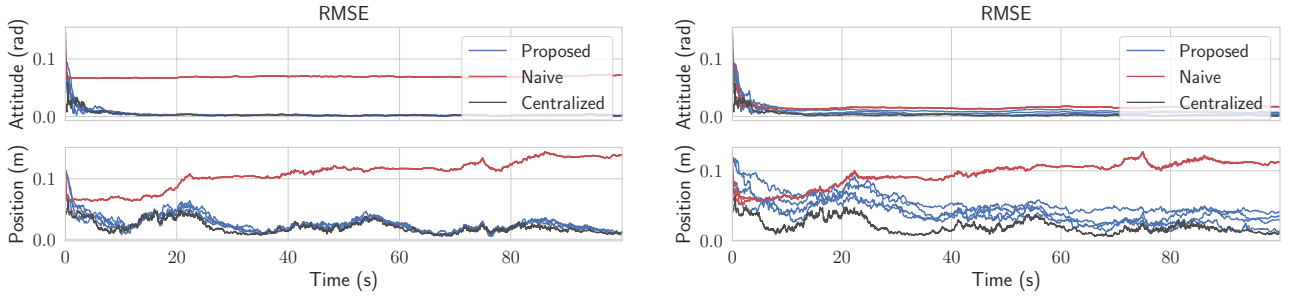


**Figure 7.** RMSE for the ground robot simulation. There are four blue lines for the four robots running the proposed algorithm, and four visibly coincident red lines for the naive algorithm. **Left:** State fusion occurring at 10 Hz. **Right:** State fusion occurring at 1Hz.

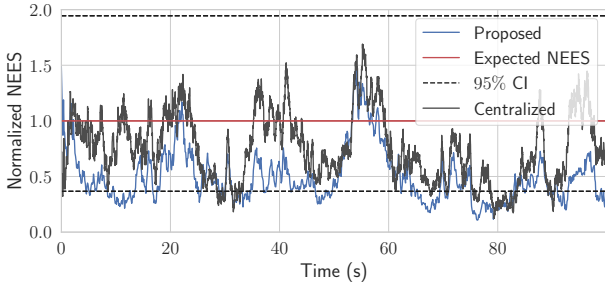


**Figure 8.** NEES plots for the ground robot simulation with 95% confidence bounds for the proposed vs. centralized solution. The naive solution without CI is far outside the plot.

## 8 Simulation and Experiments with Quadcopters

To demonstrate the flexibility of the proposed framework, consider a new problem involving quadcopters. The kinematic state of each quadcopter is modelled using extended pose matrices  $\mathbf{T} \in SE_2(3)$  (Brossard et al. (2022)). Each robot estimates both their absolute pose relative to the world frame  $\mathbf{T}_{wi} \in SE_2(3)$ , their own IMU bias  $\mathbf{b}_i$ , as well as the *relative* poses of their neighbors  $\mathbf{T}_{ij} \in SE_2(3)$  and their IMU bias  $\mathbf{b}_j$ . The full state of Robot  $i$  is then given by

$$\mathcal{X}_i = (\mathbf{T}_{wi}, \mathbf{b}_i^{[z]}, \mathbf{T}_{ij}, \mathbf{b}_j^{[z]}, \dots), \quad j \in \mathcal{N}_i.$$

The pose of Robot  $j$  relative to Robot  $i$   $\mathbf{T}_{ij}$  has kinematics involving the IMU measurements of both robots, and are given in discrete time by

$$\mathbf{T}_{ij_k} = \mathbf{U}_{i_{k-1}}^{-1} \mathbf{T}_{ij_{k-1}} \mathbf{U}_{j_{k-1}},$$

where  $\mathbf{U}_{j_{k-1}}$  has an identical definition as in (18), but computed from Robot  $j$ 's IMU measurements. When Robot  $i$  receives input measurements from its own IMU  $\mathbf{u}_k$ , it predicts the part of its own state corresponding to its own pose, and additionally performs a partial prediction on the relative poses with

$$\tilde{\mathcal{X}}_{i_k} = (\mathbf{G}_{k-1} \mathbf{T}_{wi_{k-1}} \mathbf{U}_{i_{k-1}}, \mathbf{b}_{i_{k-1}}^{[z]}, \mathbf{U}_{i_{k-1}}^{-1} \mathbf{T}_{ij_{k-1}}, \mathbf{b}_{j_{k-1}}^{[z]}, \dots).$$

The terms  $\tilde{\mathcal{X}}_{ij_{k-1}} \triangleq \mathbf{U}_{i_{k-1}}^{-1} \mathbf{T}_{ij_{k-1}}$ , which are the partially-predicted neighbor poses, are a strange, non-physical intermediate state. Only when the neighbor's RMI  $\Delta \mathbf{U}_{j_{pq}}$  is received do the neighbor poses regain meaning with  $\mathbf{T}_{ij_q} =$

$\tilde{\mathcal{X}}_{ij_p} \Delta \mathbf{U}_{j_{pq}}$ . However, since biases are also being estimated in this problem, Robot  $i$  must first correct the neighbor's raw RMIs  $\Delta \mathbf{U}_{j_{pq}}(\mathbf{u}_{j_{p:q-1}}, \mathbf{0})$  using its estimate of the neighbor's IMU bias, as described in Section 6.2. That is,

$$\Delta \mathbf{U}_{j_{pq}} \approx \Delta \mathbf{U}_{j_{pq}}(\mathbf{u}_{j_{p:q-1}}, \mathbf{0}) \oplus \mathbf{B}_{j_{pq}} \mathbf{b}_{j_q}^{[z]},$$

leading to the full state update given by

$$\mathcal{X}_{i_q} = (\mathbf{T}_{wi_q}, \mathbf{b}_q^{[z]}, \tilde{\mathcal{X}}_{ij_p} \Delta \mathbf{U}_{j_{pq}}, \mathbf{b}_{j_q}^{[z]}, \dots).$$

Finally, the pseudomeasurements chosen for this problem are

$$\mathbf{c}_{ij}(\mathcal{X}_i, \mathcal{X}_j) = \begin{bmatrix} \text{Log}(\mathbf{T}_{wi} \mathbf{T}_{ij} \mathbf{T}_{wj}^{-1}) \\ \text{Log}(\mathbf{T}_{ij} \mathbf{T}_{ji}) \\ \mathbf{b}_i^{[z]} - \mathbf{b}_j^{[z]} \\ \mathbf{b}_j^{[z]} - \mathbf{b}_i^{[z]} \\ \text{Log}(\mathbf{T}_{ij} \mathbf{T}_{j\ell} \mathbf{T}_{i\ell}^{-1}) \\ \vdots \end{bmatrix}, \quad \ell \in \mathcal{N}_i \cap \mathcal{N}_j.$$

### 8.1 Simulation Results

The algorithm is first tested with simulated versions of the described quadcopters, and the estimation results for Robot 3's absolute pose and bias are shown in Figure 9. Although there are many other states associated with the simulation, these states are the most interesting as they are the ones that are unobservable without incorporation of the pseudomeasurements. Figure 9 shows that Robot 3 is capable of estimating its own absolute pose and bias, using information from sensors located on Robots 1 and 2. Furthermore, the errors remain within the 3-sigma confidence bounds, even with the first-order RMI bias correction, indicating statistical consistency.

### 8.2 Hardware Setup

The hardware setup in these experiments can be seen in Figure 10. Three Uvify IFO-S quadcopters are used that each possess an IMU at 200Hz, a 1D LIDAR height sensor at 30Hz, and magnetometers at 30Hz. Additionally, two ultra-wideband (UWB) transceivers are installed on the quadcopter legs, producing inter-robot distance measurements at 90Hz for each robot. The UWB transceivers are custom-printed modules that use the DW1000 UWB transceiver. The firmware for these modules



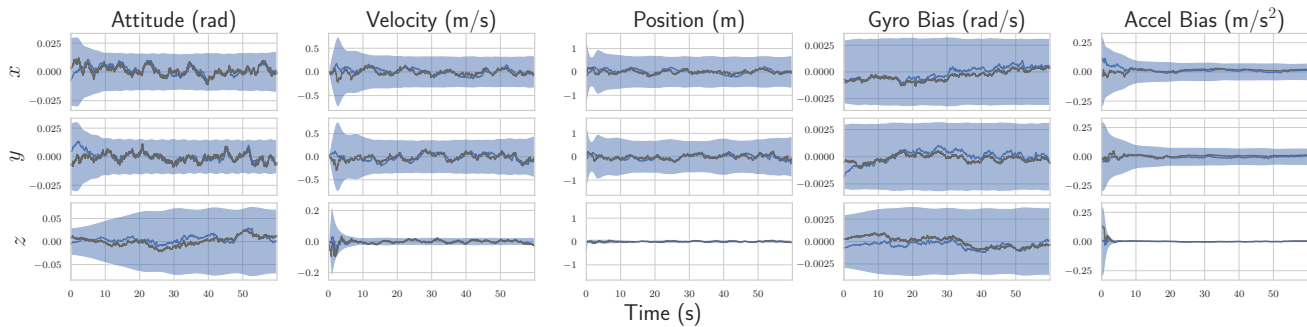


**Figure 9.** Simulated estimation error of Robot 3's estimate of its own kinematic state and IMU biases. The estimate and corresponding bounds with the proposed algorithm are shown in blue, with the centralized estimate overlaid in dark grey. For attitude, the  $x - y - z$  components represent roll-pitch-yaw errors respectively. Note that Robot 3 does not have GPS measurements, and therefore cannot observe the states shown in this plot without information sharing. The naive solution has rapidly diverging error and is not plotted.

**Table 1.** Self- Positioning RMSE (m) from experimental trials.

| Trial # | Centralized |         |         | Proposed |         |         | Error Reduction |         |         |
|---------|-------------|---------|---------|----------|---------|---------|-----------------|---------|---------|
|         | Robot 1     | Robot 2 | Robot 3 | Robot 1  | Robot 2 | Robot 3 | Robot 1         | Robot 2 | Robot 3 |
| 1       | 0.43        | 0.49    | 0.55    | 0.22     | 0.22    | 0.61    | -48%            | -54%    | 10%     |
| 2       | 0.18        | 0.26    | 0.34    | 0.16     | 0.18    | 0.40    | -13%            | -28%    | 16%     |
| 3       | 0.17        | 0.24    | 0.68    | 0.16     | 0.17    | 0.45    | -10%            | -28%    | -33%    |
| 4       | 0.20        | 0.25    | 0.31    | 0.26     | 0.28    | 0.48    | 32%             | -13%    | 55%     |

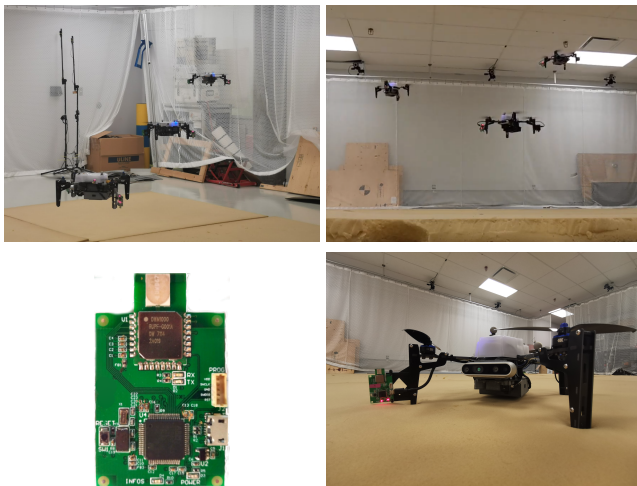


**Figure 10.** **Top:** Three quadcopters in flight under a motion capture system. **Bottom left:** our custom UWB module. **Bottom right:** a close up of the Uvify IFO-S quadcopter, fitted with a UWB module seen on the left leg, as well as on the opposite leg.

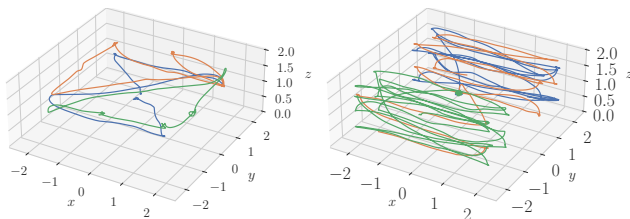


**Figure 11.** Examples of the various trajectories flown in the experimental trials, where each color represents a different quadcopter.

has been written in C, implementing a double-sided two-way-ranging protocol with details described by [Shalaby et al. \(2022\)](#). [Shalaby et al. \(2022\)](#) also describe the power-based bias calibration and noise characterization procedure used in these experiments. Since all transceivers operate on the same frequency in these experiments, only one can transmit at a time to avoid interference. A decentralized scheduler is therefore implemented that continuously cycles through all transceiver pairs one at a time, obtaining range measurements and potentially transmitting other useful data.

A Vicon motion capture system is used to collect ground truth, from which synthesized GPS measurements with a standard deviation of 0.3 m are generated for Robots 1 and 2 only. Robot 3 does not possess GPS measurements, nor any magnetometer measurements, and therefore has no absolute pose information available without communication with the other two robots. Example trajectories for some of the experimental trials are shown in [Figure 11](#).

### 8.3 Experimental Results

Multiple experimental runs are performed on different days, with the absolute positioning results for each robot viewable in [Table 1](#). In some cases, the proposed algorithm even outperforms the centralized solution, which is theoretically optimal. However, the real world contains many unmodelled sources of error, such as frame misalignments, timestamping errors, vibrations, and UWB ranging outliers. Even after substantially increasing the datasheet-provided covariances associated with the IMU measurements, it appears that the results benefit from the covariance inflation resulting from CI. For both estimators, the IMU is calibrated to compensate for large biases and scaling factors. The normalized-innovation-squared test ([Bar-Shalom et al. \(2001\)](#)) is also used to reject UWB outliers in both estimators,

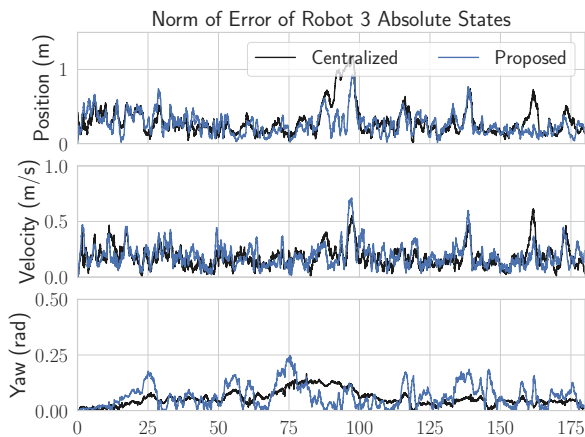


**Figure 12.** Position, velocity, and yaw RMSE for Robot 3 from one of the experimental trials. Since Robot 3 has no GPS, these quantities are unobservable without the fusion of pseudomeasurements.

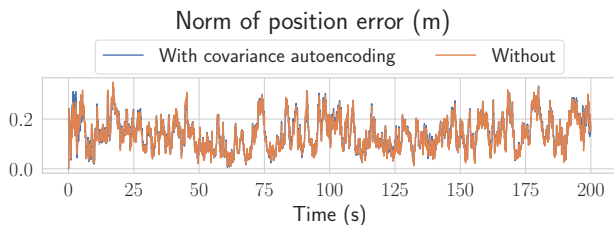


**Figure 13.** The effect of preintegrated covariance autoencoding, as described in Section 6.3, on the position estimate of Robot 1. The two lines are almost identical, showing that the proposed autoencoder induces minimal error on the estimate. All other states have similar plots.

A plot of RMSE versus time for Robot 3’s absolute states can be seen in Figure 12, which are states that are unobservable from Robot 3’s own measurements. Again, Figure 12 shows that error magnitudes lie in similar ranges for both the centralized and decentralized estimators. Figure 13 compares two decentralized estimator runs, with one using the mean-assisted autoencoder from Section 6.3. As desired, the lines are identical, and the plot shows that the estimate is unaffected by the autoencoding. This means that the autoencoder is highly effective at compressing the covariance matrix with minimal reconstruction error.

## 9 Conclusion

This paper presents a general-purpose algorithm for decentralized state estimation in robotics. The algorithm is the result of a new way to formulate the decentralized state estimation problem, specifically with the assistance of pseudomeasurements that allow the definition of arbitrary non-linear relationships between robot states. The algorithm is tested on three different problems, each involving a variety of state definitions, process models, and measurements. Thanks to covariance intersection, the algorithm is appropriate for arbitrary, potentially time-varying graphs, and does not require any bookkeeping, growing memory, buffering of measurements, or reprocessing of data. At the same time, the approximation made by covariance intersection makes

the proposed method suboptimal, as it is well-known to be overly-conservative. Nevertheless, in the specific problems shown in this paper, the results using CI have been satisfactory provided that the fusion frequency is high enough, and the communication graph is not too sparse.

Future work can consider improving the approximation made by CI. Also, using the proposed MAP approach with pseudomeasurements, it should be possible to derive decentralized batch and sliding-window estimators, often termed *smoothers*, since these algorithms also originate from the MAP problem.

## Funding

This work was supported by the NSERC Alliance Grant program, the NSERC Discovery Grant Program, the CFI JELF program, and by the FRQNT.

## Acknowledgements

The authors would like to thank Justin Cano and Jérôme Le Ny for their assistance in the development of custom UWB modules.

## References

- Allak E, Barrau A, Jung R, Steinbrener J and Weiss S (2022) Centralized-Equivalent Pairwise Estimation with Asynchronous Communication Constraints for two Robots. In: *Intl. Conf. on Intelligent Robots and Systems*. pp. 8544–8551.
- Allak E, Jung R and Weiss S (2019) Covariance Pre-Integration for Delayed Measurements in Multi-Sensor Fusion. In: *Intl. Conf. on Intelligent Robots and Systems*. pp. 6642–6649.
- Bar-Shalom Y, Li XR and Kirubarajan T (2001) *Estimation with Applications to Tracking and Navigation*. New York: John Wiley & Sons, Inc.
- Barfoot TD (2023) *State Estimation for Robotics*. 2nd edition. Cambridge University Press.
- Barfoot TD and Furgale PT (2014) Associating Uncertainty with Three-Dimensional Poses for use in Estimation Problems. *IEEE Trans. on Robotics* 30(3): 679–693.
- Battistelli G, Chisci L, Mugnai G, Farina A and Graziano A (2015) Consensus-Based Linear and Nonlinear Filtering. *IEEE Trans. on Automatic Control* 60(5): 1410–1415.
- Brossard M, Barrau A, Chauchat P and Bonnabel S (2022) Associating Uncertainty to Extended Poses for on Lie Group IMU Preintegration With Rotating Earth. *IEEE Trans. Robotics* 38(2): 998–1015.
- Carrillo-Arce LC, Nerurkar ED, Gordillo JL and Roumeliotis SI (2013) Decentralized multi-robot cooperative localization using covariance intersection. *IEEE Int. Conf. Intell. Robot. Syst.* : 1412–1417.
- Forster C, Carlone L, Dellaert F and Scaramuzza D (2017) On-Manifold Preintegration for Real-Time Visual-Inertial Odometry. *IEEE Trans. Robotics* 33(1): 1–21.
- Grime S and Durrant-Whyte HF (1994) Data fusion in decentralized sensor networks (Information Filter). *Control Engineering Practice* 2(5): 849–863.
- Julier S (2001) General Decentralized Data Fusion with Covariance Intersection (CI). In: *Multisensor Data Fusion*, chapter 12. pp. 269–294.

- Julier SJ and Uhlmann JK (1997) A non-divergent estimation algorithm in the presence of unknown correlations. In: *American Control Conference*, volume 4. pp. 2369–2373.
- Jung R, Brommer C and Weiss S (2020) Decentralized Collaborative State Estimation for Aided Inertial Navigation. In: *Intl. Conf. on Robotics and Automation*. pp. 4673–4679.
- Leung KY, Barfoot TD and Liu HH (2010) Decentralized localization of sparsely-communicating robot networks: A centralized-equivalent approach. *IEEE Trans. Robotics* 26(1): 62–77.
- Leung KY, Barfoot TD and Liu HH (2012) Decentralized cooperative SLAM for sparsely-communicating robot networks: A centralized-equivalent approach. *J Intell. and Robot Syst.* 66(3): 321–342.
- Li L and Yang M (2021) Joint localization based on split covariance intersection on the lie group. *IEEE Trans. Robotics* 37(5): 1508–1524.
- Luft L, Schubert T, Roumeliotis SI and Burgard W (2018) Recursive decentralized localization for multi-robot systems with asynchronous pairwise communication. *Intl Journal of Robotics Research* 37(10): 1152–1167.
- Lupton T and Sukkarieh S (2012) Visual-inertial-aided navigation for high-dynamic motion in built environments without initial conditions. *IEEE Trans. Robotics* 28(1): 61–76.
- Olfati-Saber R (2005) Distributed Kalman filter with embedded consensus filters. *IEEE Conf. Decis. Control. Eur. Control Conf.* : 8179–8184.
- Olfati-Saber R and Murray RM (2004) Consensus problems in networks of agents with switching topology and time-delays. *IEEE Trans. on Automatic Control* 49(9): 1520–1533.
- Psiaki ML (2013) The blind tricyclist problem and a comparative study of nonlinear filters: A challenging benchmark for evaluating nonlinear estimation methods. *IEEE Control Systems Magazine* 33(3): 40–54.
- Roumeliotis SI and Bekey GA (2002) Distributed multirobot localization. *IEEE Trans. Robotics and Auto.* 18(5): 781–795.
- Shalaby M, Cossette CC, Forbes JR and Le Ny J (2023) Multi-Robot Relative Pose Estimation and IMU Preintegration Using Passive UWB Transceivers (preprint) URL <https://arxiv.org/abs/2203.11004>.
- Shalaby M, Cossette CC, Le Ny J and Forbes JR (2021) Cascaded Filtering Using the Sigma Point Transformation. *IEEE Robotics and Automation Letters* .
- Shalaby MA, Cossette CC, Forbes JR and Ny JL (2022) Calibration and Uncertainty Characterization for Ultra-Wideband Two-Way-Ranging Measurements (preprint). URL <https://arxiv.org/abs/2210.05888v2>.
- Solà J, Deray J and Atchuthan D (2018) A Micro Lie Theory for State Estimation in Robotics. URL <http://arxiv.org/abs/1812.01537>.